ifenprodil. These observations indicate that PSA and PSA-NCAM interact with the NR2B containing NMDA receptors. However, in the hippocampus, synaptic NMDA receptors contain NR2A and extrasynaptic NMDA receptors contain NR2B (47), which causes loss of mitochondrial membrane potential (an early marker for glutamate-induced neuronal damage) and cell death. These results raise doubt about whether the effect of PSA-NCAM on NR2B is involved in synaptic plasticity. On the other hand, a report found that post-synapses contain NR2B, which affects the induction of LTP in the amygdala which receives projections from the hippocampus (48). Therefore, also in the hippocampus, the effect of PSA-NCAM on NR2B may be directly involved in NMDAR-dependent LTP.

PSA expressed dependent on ST8Sia IV is necessary for the induction of LTP and LTD in the CA3-CA1 synapse of only adult mice (more than 4 weeks old) (43). The abundant expression of ST8Sia II in newborn mouse brain shifts toward a prominent expression of ST8Sia IV in the adult brain (49). This expressional shift might affect differences between juveniles and adults concerning the acquirement of synaptic plasticity.

Furthermore, previous reports have shown the involvement of PSA-NCAM in higher neural plasticity. In a fear-conditioning test suitable for observations of emotional stress (45), the injection of PSA-NCAM-Fc into the hippocampus *in vivo* resulted in a reduction of freezing time when the mice entered a room where they had previously received footshocks (contextual learning). On the other hand, NCAM-deficient mice have a disturbed contextual memory. The mice received an injection of PSA-NCAM-Fc or NCAM-Fc into the hippocampus, resulting in an extension of or no effect on the freezing time, respectively. As these effects of PSA-NCAM do not occur following an injection into the amygdala, an adequate dose of PSA in the hippocampus seems to be involved in emotional stress. The suprachiasmatic nuclei (SCN) of the hypothalamus contain an endogenous circadian clock that maintains synchrony with the external environment through light input and express PSA-NCAM. In rat brain slices recorded for 3 days, the mean firing frequency of SCN neurons was recorded as a sinusoidal curve over a 24 hour period with a peak at midday, resembling the circadian rhythm, and treatment of the slices with glutamate produced light-like shift of 3 hours in the circadian rhythm (54). On the other hand, in NCAM-180-deficient mice, circadian rhythmicity was abolished, resulting from a determination based on activity in darkness (55). Furthermore, treatment with Endo-N in the SCN disturbs the light-like shift caused by glutamate (53). These results suggest that PSA affects circadian rhythm and is also relevant to synaptic plasticity via glutamate stimulation. Additionally, several reports have

がNR2Bに作用することがわかってきた(46)。細胞外に添加したPSAやPSA-NCAMがグルタミン酸刺激による単一のNMDARチャネル活性を阻害するものである。またNR2B特異的阻害剤（ifenprodil）が、PSAやPSA-NCAMによるチャネル活性阻害と競合することから、PSAやPSA-NCAMが、NR2Bに作用することが明らかとなった。しかしながら、海馬ニューロンのシナプスNMDARがNR2Aであり、シナプス外NMDARがNR2Bであるという報告があること(47)、さらには、NR2B阻害がグルタミン酸刺激による細胞死を抑制することから、NR2Bを介したPSA-NCAMの作用がシナプス可塑性に直接関与するかどうかは、議論の残すところがある。しかしながら最近、海馬に入力繊維を持つ扁桃体において、NR2Bがスパイン（後シナプス）に存在し、LTPに関与する知見が報告された(48)。それ故、CA1シナプスにおいてもNR2Bを介したNMDAR-dependent LTPが存在し、PSAやPSA-NCAMが関与している可能性も残されている。

加えて、CA3-CA1シナプスにおけるLTP及びLTDに関わるPSAは、ST8Sia IVによるポリシアル酸転移によるようである(43)。ただしそれは4週齢以降のマウスにおいて観察された結果で、2週齢のST8Sia IV欠失マウスでは影響がない。これは、ST8Sia IIが発生期に強く発現し、出生後成熟するにつれてST8Sia IVの発現に移行することに反映されていると思われる(49)。すなわち、シナプス可塑性の獲得方法が幼弱期と成熟期の間で異なり、PSAの関わり方も変化すると考えられる。

さらにPSA-NCAMについては、高次の神経可塑性への関与を示唆する報告がある。例えば、情動ストレスの観察に適した恐怖条件付けストレスを与えたマウスの海馬内へ、PSA-NCAM-Fcを注入した後、電気ショックを受けた部屋に再び入れるとfreezing時間が短縮する。その一方で、NCAM欠失マウスはもともとfreezinig時間が短く、海馬にPSA-NCAM-Fcを注入するとfreezing時間が延長するが、NCAM-Fcでは効果がない。これは海馬におけるPSA量の調整が、情動ストレスに関与していることを示している。さらに扁桃体への注入ではfreezinig時間に影響を与えないことから、海馬に特異的なシナプス可塑性の高次機能を示していると考えられる(45)。またPSAは、サーカディアンリズムの獲得にも寄与していることが知られている(53)。視床下部視交叉上核(SCN)が、外界からの明暗信号を受け取ることによりサーカディアンリズムの同調が生じる。In vitro SCNスライスに記録電極を入れると、発火周波数が正弦曲線を描く明期にあたる時間（明期様）と、正弦曲線を描かない暗期にあたる時間（暗期様）からなる、24時間の日周リズムが得られる（3日間生存時のリズムをきざむ）。そして暗期にグルタミン酸を投与すると、明期に見られる周波数のピークが3時間移相する事が知られている（54)。NCAM-180欠失マウスでは、明暗期における運動活性のリズムが同調しなくなること（明期は睡眠、暗期は活動）が明らかになり(55)、さらにはSCNスライスにおけるグルタミン酸刺激による周波数ピークの3時間移相が、Endo-N処理により阻害されることから、PSAの発現がSCNのサーカディアンリズムに関与し、グルタミン酸を介するシナプス可塑性との関

proposed effects of PSA on neural plasticity via neuronal hormones: lactation by stimulation with oxytocin in supraoptic nuclei of the hypothalamus (56), estradiol-induced increase in the number of GABAergic axo-somatic synapses in the arcuate nucleus of the hypothalamus (57), and developmental migration of neurons expressing luteinizing hormone-releasing hormone (LHRH) (58) and so on. Other reports have also suggested that PSA has relevance to neuronal diseases including epilepsy (59, 60), heroin addiction (61), and the proliferation of neural stem cells (62).

D. HNK-1

The carbohydrate HNK-1 is carried by glycolipids and glycoproteins including the immunoglobulin (Ig) superfamily (NCAM, P0, L1, and F3/F11/contactin), integrin, proteoglycans, and the extracellular matrix glycoproteins (tenascin-C, -R). HNK-1 is involved in neural development and synaptic plasticity through the mediation of cell-cell recognition. HNK-1 is a sulfated trisaccharide (HSO_3-3GlcAβ1-3Galβ1-4GlcNAc) and two glucuronyltransferases (GlcAT-P, GlcAT-S) and one sulfotransferase (HNK-1ST) are involved in its biosynthesis. Studies have been conducted with GlcAT-P and HNK-1ST deficient mice to know whether HNK-1 is involved in neural plasticity (63,64). Deficiencies of both GlcAT-P and HNK-1ST resulted in an inhibition of LTP in the CA3-CA1 synapse, suggesting the involvement of HNK-1 in synaptic plasticity. The molecular mechanism of LTP via HNK-1 needs to be analyzed in more detail. On the other hand, it has been reported that the application of anti-HNK-1 antibody induced an increase of LTP and decrease of $GABA_A$ receptor-mediated pIPSCc (perisomatic inhibitory postsynaptic currents) in CA3-CA1 synapses (65). HNK-1 antibody did not affect pIPSCs in knock-out mice deficient in tenascin-R, but did affect them in NCAM-deficient mice. These results provide evidence that HNK-1 carried by tenascin-R is involved in channel permeability of $GABA_A$ receptor at least in some hippocampal neurons.

E. Fucα(1-2)Gal

Fucose-α(1-2)-galactose [Fucα(1-2)Gal], which exists as a terminal carbohydrate modification to N- and O-linked glycoproteins, has been implicated in learning and memory (66,67). 2-deoxy-D-galactose (2-dGal) prevents the formation of Fucα(1-2)Gal linkages by incorporation of the drug into glycan chains, reversibly. On injection of 2-dGal into the rat intra vein, STP and LTP which should be induced by high frequency stimulation are interfered with in the EC-DG synapse (perforant pathway) and CA3-CA1 synapse (Schaffer collateral) (68). Also, the injection of an antibody (A46-B/B10) recognizing the Fucα(1-2)Gal epitope impaired the retention performance of rats in a relearning session with

連性が示唆される (53)。この他 PSA は、オキシトシン刺激による泌乳刺激時における視床下部視索上核 (SON) における反応 (56)、エストロゲン刺激による抑制性ニューロンシナプス数の制御 (57)、さらには、黄体形成ホルモン放出ホルモン発現ニューロンの発生時の遊走 (58) 等、神経ホルモンに関わる可塑的変化への関与を示唆する報告がある。またてんかん形成 (59、60) やヘロイン中毒 (61) 等の疾患や、神経幹細胞の増殖 (62) との関連性の可能性を示唆する論文も報告されており、今後のさらなる研究の進展が望まれる。

D. HNK-1

HNK-1 糖鎖は、糖脂質あるいは、イッムノグロブリン (Ig) スーパーファミリー (NCAM, P0, L1, F3/F11/contactin) やインテグリン , プロテオグリカン , 細胞外マトリクス tenascin-C, tenascin-R 等の糖タンパク質に付加する糖鎖で、細胞間認識機構を利用した神経発生やシナプス可塑性に関与する。この HNK-1 は、N- アセチルラクトサミン構造の非還元末端に存在するガラクトース残基にグルクロン酸を転移する 2 種のグルクロン酸転移酵素 (GlcAT-P, GlcAT-S) と硫酸基を転移する硫酸基転移酵素 (HNK-1ST) より合成され、近年 GlcAT-P と HNK-1ST のノックアウトマウスが作成され、シナプス可塑性について調べられている。共に CA3-CA1 シナプスにおける LTP の抑制が観察され、HNK-1 のシナプス可塑性への関与が示唆された (63、64)。この LTP への関与に関する分子メカニズムは今後の解析を待つところである。しかしながら、HNK-1 抗体が、CA3-CA1 シナプスの LTP を上昇させると共に、$GABA_A$ 受容体由来の pIPSC の振幅を低下させた報告がある (65)。この pIPSC は、NCAM 欠失マウス海馬でも、野生型と同様に観察されたが、tenascin-R 欠失マウス海馬ではおこらなかった。これは、tenascin-R に付加された HNK-1 が、少なくとも一部の海馬ニューロンの $GABA_A$ 受容体のチャネル透過性に関わっている事を示している。

E. Fuc α (1-2)Gal

Fuc α (1-2)Gal は、N- 結合型、O- 結合型糖タンパク質の糖鎖の末端に付加され、学習記憶に関わることが以前より示唆されてきた (66、67)。2-deoxy-D-galactose (2-dGal) は、脳での Fuc α (1-2)Gal 残基形成を阻害する試薬である。例えばあらかじめ電極を挿入したラットの尾静脈に 20 μ mol 2-dGal 注入 30 分後、EC-DG シナプス (貫通繊維路) 及び CA3-CA1 シナプス (シャファー側枝) に高頻度刺激をおこなったところ、STP の抑制が観察され、その後の追加 (20 μ mol) により、LTP の誘導も抑制された (68)。また Fuc α (1-2)Gal エピトープを認識する抗体 (A46-B/B10) を海馬内に注入後、情動ストレス学習 (明暗箱のうち暗所に入るとフットショックが誘導される passive

passive avoidance, which is a method of determining the effect on learning of an unpleasant stimulus [When rat enters a dark alley, rat is punished by footshocks despite preference for dark](69). Many reports implicate Fucα(1-2)Gal in amnesia with behavioral analyses.

Finally, it was recently clarified that the carrier of Fucα(1-2)Gal is synapsin Ia and Ib (70). The A46-B/B10 antibody recognizes synapsin. The addition of 2-dGal to cells prevents the fucosylation of synapsin, resulting in synapsin's degradation mediated by the calcium-dependent protease calpain. The de-fucosylation changes the cellular half-life of synapsin from 18 to 5.5 hours.

Synapsin tethers synaptic vesicles to the actin cytoskeleton. An increase of $[Ca^{2+}]i$ activates PKA (protein kinase A) and CaM kinase, resulting in phosphorylation of synapsin. Then, phosphorylated synapsin withdraws its role as a tether and synaptic vesicles prepare to dock and fuse with the active zone of the presynaptic membrane, resulting in the release of neurotransmitters. Therefore, a steady supply of synapsin is very important to the acquirement of synaptic plasticity and Fucα(1-2)Gal bears the primary responsibility for the stability of synapsin.

F. Proteoglycan

Proteoglycans are heavily *O*-glycosylated proteins. The carbohydrate structure is called glycosaminoglycan (GAG) and composed of repeating disaccharide units: amino sugar derivatives and hexose derivatives, with diversity in the position and quantity of sulfation. Proteoglycans are secreted into the extracellular matrix and inserted into the plasma membrane, and influence cell-environment interactions by binding to a heterogeneous group of growth factors and other matrix ligands, and adhesion molecules. In the central nervous system, hyaluronan, chondroitin sulfate, and heparan sulfate among proteoglycans, especially, influence the development of neural circuits and regeneration of neural injury (71–73). Furthermore, the involvement of chondroitin sulfate and heparan sulfate in synaptic plasticity has been reported.

F-1. Chondroitin Sulfate

Treatment with chondroitinase ABC of hippocampal slices resulted in the disappearance of LTP or LTD in the CA3-CA1 synapse (Schaffer collateral) (74). On the other hand, it has been reported that tenascin-R binds with chondroitin sulfate and the CA3-CA1 synapse of tenascin-R-deficient mice exhibits a reduction of LTP compared to the wild type (75). The degree of the reduction is the same with or without chondroitinase ABC, suggesting that binding between tenascin-R and chondroitin sulfate is involved in the development of LTP. On the other hand, there is no effect in tenascin-R-deficient mice on LTD in the CA3-CA1 synapse, showing that the effect of chondroitinase ABC on LTD is

avoidance を用いており、ラットは暗所を好むことから、不快刺激の学習効果をみるもの。）を行ったところ、学習効果が減弱したことから、海馬依存の空間認知記憶が傷害されていることがわかった (69)。以上のことから、Fuc α (1-2)Gal は健忘症関連糖鎖であると認知されていた。

最近になって、Fuc α (1-2)Gal の主要担体が synapsin Ia と Ib であることが判明した (70)。その発端は先に用いた A46-B/B10 抗体が、シナプシンを認識したことにある。そして、シナプシンは 2-dGal を取り込むことにより、Fuc α (1-2)Gal 残基を持たなくなり、その結果、カルパイン (calcium-dependent protease calpain) に分解されるようになり、Fuc α (1-2)Gal を持たないシナプシンの半減期は、18 時間から 5.5 時間へと減少する。

シナプス小胞は、シナプシンを介してアクチン繊維につなぎ止められており、シナプス前終末の脱分極により細胞内に Ca^{2+} が流入することで、PKA や CaM kinase が活性化され、シナプシンはリン酸化される。シナプシンがリン酸化されるとシナプス小胞はアクチン繊維から遊離し、シナプス前膜のアクティブゾーンにドッキングし、神経伝達物質の放出を待つ。このことから、シナプシンの安定供給は、シナプス可塑性の獲得にとって非常に重要であることがわかり、Fuc α (1-2)Gal 修飾が、シナプシンの安定化を担っていることが明らかとなった。

F. プロテオグリカン

プロテオグリカンは O- 結合型糖タンパク質で、糖鎖部分はグリコサミノグリカンと呼ばれ、アミノ糖とウロン酸の 2 糖単位の繰り返し構造からなり、硫酸基の修飾の位置と程度により多様性を持つ。プロテオグリカンの多くは、細胞外マトリクスに含まれ、他の細胞外マトリクスや細胞接着因子と結合し、細胞間コミュニケーションや、細胞間の空間維持に関与している。中枢神経系では、これまで脳の神経回路発達や中枢神経損傷後の修復に、ヒアルロン酸、コンドロイチン硫酸、ヘパラン硫酸の関与が明らかになってきている (71–73)。さらにプロテオグリカンの中でも、特にコンドロイチン硫酸、ヘパラン硫酸がシナプス可塑性に関与することが知られており、本稿では、このシナプス可塑性への関与について解説する。

F-1. コンドロイチン硫酸

海馬をコンドロイチナーゼ ABC 処理によりコンドロイチン硫酸を分解した後、CA3-CA1 シナプス（シャファー側枝）に高頻度刺激をおこなったところ、LTP 及び LTD が抑制された (74)。一方、以前より LTP に関与する細胞外マトリクスでコンドロイチン硫酸に結合する分子が tenascin-R であることが知られていた (75) ことから、tenascin-R 欠失マウス海馬への ABC 処理の効果を見たところ、ABC 処理前後 LTP 抑制効果は同じであった。この結果は、少なくともコンドロイチン硫酸の tenascin-R との結合が LTP の発生に関与していることを示唆している。一方で、tenascin-R 欠失マウス海馬は LTD の影響がみられないことから、ABC 処理による LTD 効果は、

induced by the binding of chondroitin sulfate to a component of the extracellular matrix other than tenascin-R. Furthermore, mice deficient in Ptprz (protein tyrosine phosphatase receptor type Z), having domains for binding with chondroitin sulfate, also showed a reduction of LTP compared to wild-type mice in the CA3-CA1 synapse (76). These results suggest that chondroitin sulfate binds with Ptprz, tenascin-R, HNK-1, and so on extracellularly and seems to coordinate synaptic plasticity.

The involvement of brevican and NG2, proteoglycans containing chondroitin sulfate, in synaptic plasticity has been reported. First, brevican-deficient mice showed significant deficits in the maintenance of LTP in the CA3-CA1 synapses of hippocampal slices. Additionally, application of anti-brevican antibody also shows deficits in the LTP in the CA3-CA1 synapse (77). Alternatively, NG2 is expressed in 5 to 10 % of all cells, depending on the brain region, especially in the hippocampus. NG2-positive cells are glia that do not express GFAP (glial fibrillary acidic protein) or MBP (myelin basic protein). NG2-positive cells are not astrocytes or oligodendrocytes. Furthermore, the neuron-glia synapse is found in NG2-positive cells (78). Ge *et al.* made whole-cell recordings from NG2 cells in the CA1 region of rat hippocampal slices by inducing glial cell membrane currents with a high frequency stimulation of Schaffer collaterals (79). The identity of astrocytes and NG2 cells was determined by post-immunostaining. Theta burst stimulation resulted in a persistent increase in the EPSC (excitatory postsynaptic current) amplitude in NG2 cells, analogous to LTP found in synaptic plasticity existing between neurons. The LTP-like EPSCs were reduced by philanthotoxin-33, a toxin that specifically blocks the CaPARs (Ca^{2+}-permeable AMPA receptors), Kyn (NMDA, quisqualate, and kainite receptor blocker), and BAPTA (calcium cannel chelator). These results show that NG2 cells induce a NMDAR-independent LTP that depends on $[Ca^{2+}]i$. Further research is needed to know whether NG2 itself is implicated in synaptic plasticity, however, the involvement of NG2-positive cells in synaptic plasticity has been clarified.

F-2. Heparan Sulfate

Among proteoglycans with heparan sulfate, syndecan-3 is expressed in pyramidal cells in the CA1 subfield of the hippocampus and biological analyses show that FGF and HB-GAM bind syndecan-3 in the hippocampus. Two approaches have been used to investigate the effects of heparan sulfate on the induction and maintenance of LTP. First, treatment with heparitinase of hippocampal slices resulted in the disappearance of LTP in the CA3-CA1 synapse (Schaffer collateral) (34,80). Second, the application of a soluble syndecan-3 to hippocampal slices prevented LTP in the CA3-CA1 synapse. On the other hand, syndecan-3-deficient mice

tenascin-R 以外の細胞外マトリクスとの相互作用が影響していると思われる。また一方で、コンドロイチン硫酸接着領域を持つ Ptprz(protein tyrosine posphatase receptor type Z) の欠失マウス成熟海馬スライスの CA3-CA1 シナプス（シャファー側枝）に高頻度刺激をおこなったところ、LTP が抑制され、これも NMDA-independent LTP であった (76)。以上の結果より、コンドロイチン硫酸は、Ptprz, tenascin-R、HNK-1 などと共に細胞外で結合し合い、シナプス可塑性を調整しているのであろう。

一方で、コンドロイチン硫酸を持つプロテオグリカンの中で、brevican と NG2 に関するシナプス可塑性が報告されている。まず、brevican は直接 LTP に関与しているようである (77)。Brevican 欠失マウス海馬スライスは CA3-CA1 シナプス（シャファー側枝）における LTP の誘導が抑制され、さらには、コントロールマウス海馬スライスに抗 brevican 抗体を投与したところ、LTP の誘導が阻害された。一方で、NG2 に関する知見は、少し趣を異にしている。NG2 は、脳の 5-10% の細胞が発現しているが特に海馬に多く、GFAP (glial fibrillary acidic protein) 陰性及び、MBP (myelin basic protein) 陰性のグリア細胞に発現している。すなわち、一般に言われているアストロサイトでもオリゴデンドロサイトでもない細胞であり、さらに NG2 細胞は、ニューロンとシナプスを作る (78)。Ge らは、海馬スライスのシャファー側枝に LTP 誘導刺激を送り、CA1 領域に存在する NG2 細胞の膜電位をパッチクランプにより測定した (79)。NG2 細胞であるかどうかは、パッチクランプ測定後に免疫染色をおこない、個々に同定している。LTP 導入刺激 (theta burst stimulation) により、NG2 細胞は、興奮性後シナプス電流 (EPSCs) の拡大を示した。この LTP 様の反応は、Ca^{2+} 透過性 AMPA 受容体の阻害剤 (PhTx) で抑制され、さらには、Kyn(NMDA, quisqualate, and kainate receptor blocker) や、カルシウムチャネルキレート剤 (BAPTA) でも、抑制された。これらのことから、NG2 細胞は、non-NMDA 受容体依存的に LTP を誘導し、この LTP は、ニューロンーニューロン間シナプスと同様に細胞内 Ca^{2+} 濃度に依存した LTP であることが明らかとなった。実際に NG2 自身が、LTP に関与しているかどうかは、今後の検討課題ではあるが、少なくとも、NG2 を発現しているグリア細胞が、LTP 誘導に関わっていることが明らかとなった。

F-2. ヘパラン硫酸

ヘパラン硫酸を持つプロテオグリカンのうち、シンデカン -3 が海馬 CA1 錐体細胞に発現することが知られている。さらに生化学的解析より、海馬ではシンデカン -3 が細胞外で FGF や HB-GAM と結合することがわかっている。ヘパラン硫酸についても、先に示してきた方法論によりシナプス可塑性への関与について調べた知見がある。まず、海馬をヘパリチナーゼ処理によりヘパラン硫酸を分解した後、CA3-CA1 シナプス（シャファー側枝）に高頻度刺激をおこなったところ、LTP が抑制された（34,80)。また可溶性シンデカン -3 を海馬 CA1 領域に添加後 CA3-CA1 シナプスに高頻度刺激をおこなうと、LTP が抑制された。一方で、シンデカン -3 欠失マウス海馬では、

showed an increase of LTP in the CA3-CA1 synapse (81). Previous reports have indicated that FGF increases LTP (82) and HB-GAM impairs LTP (83) in the hippocampus. The heparan sulfate might coordinate the effects of FGF and HB-GAM on neural plasticity. Recent research has indicated that *Drosophila* heparan sulfate proteoglycan: syndecan and Dallylike [glycosylphosphatidylinositol (GPI) anchored glypican] play important roles in the development of synapses in neuromuscular junctions (84). It is known that boutons in presynaptic terminals contain active zones that organize glutamate's release and an increase of synaptic activity enlarges the active zone per bouton, which requires LAR family RPTPs (protein tyrosine phosphatases) (85). First, both syndecan and dallylike bind LAR. Second, the syndecan-deficient mutant shows a decrease of bouton size and the Dallylike-deficient mutant shows a decrease of active zone size. Finally, a double mutant assay showed the requirement of LAR for actions of both syndecan and Dallylike. The discovery of the collaboration of these heparan sulfate proteoglycans in morphological synaptic plasticity will lead to analyses in mammalian systems including the mouse and rat.

G. Concluding Remarks

This review focused on 5 species of carbohydrate, whose structure had been identified and for which there were knock-out mice deficient in the transferase required to synthesize the carbohydrate. There are reports that carbohydrates affect the maturation of channels, channel activity, and the transport of synaptotagmine to presynaptic terminals and so on (24,86–90) and that carbohydrates are implicated in synaptic plasticity (91–93). Furthermore, concerning the neural plasticity described in the introduction, analyses at the cellular and molecular level should progress in the near future and carbohydrates will attract more attention.

CA3-CA1 シナプスにおける LTP を亢進した (81)。以前より、海馬では FGF が LTP を亢進すること (82)、HB-GAM が LTP を抑制すること (83) が知られている。このことは、ヘパラン硫酸を介した FGF、HB-GAM、シンデカンの結合が、シナプス可塑性に何らかの関与を示していることを示唆する。最近2種のヘパラン硫酸プロテオグリカン；シンデカンと Dallylike [GPI (glycosylphosphatidylinositol) anchored glypican] が、ショウジョウバエの神経筋接合部におけるシナプス発達機構に重要な役割を示すことが報告された (84)。シナプス前終末 (bouton) はグルタミン酸放出部分である active zone を含み、シナプス活性が亢進された場合、この bouton あたりの active zone が広がる。このシナプス形成にレセプター型チロシンホスファターゼの LAR ファミリーメンバーが関与することがすでに知られている (85)。その一方で、シンデカン欠失ミュータントは、bouton の大きさを縮小し、Dallylike 欠失ミュータントは、bouton あたりの active zone の縮小を示した。さらに、生化学的解析より、シンデカン及び Dallylike が共に LAR に結合すること、LAR 欠失ミュータントとのかけあわせにより、シンデカンは LAR を促進し、Dallylike は抑制することがわかった。以上のことから、ヘパラン硫酸プロテオグリカンがシナプス前終末におけるシナプス活性に重要な役割を持つことが明らかになった。今後マウスを含む哺乳動物におけるシナプス可塑性への生理学的な解析も進むと思われる。

G. 結　語

本稿では、糖鎖が特定されているもの、ノックアウトマウスの存在あるいは分子間相互作用の知見が明らかになっているもの、に焦点を当てた。本稿で解説したような糖鎖の特定がなされていないものの中には、チャネルに付加された糖鎖が、チャネルの成熟や、チャネル活性の修飾に関与する例 (24、86–89) や、シナプス前終末へのシナプトタグミンの配置に糖鎖が関与する例 (90) 等、糖鎖がシナプス可塑性に関与する例が多く報告されている (91–93)。序論で述べたような複雑な神経可塑性に関しても、今後分子レベルに及ぶ研究が進み、糖鎖の重要性がさらに注目されてくるであろう。

Reference

1. Hyde, P. S., and Knudsen, E. I. (2002) Nature **415**, 73–76
2. Squire, L. R., Bloom, F. E., McConnell, S. K., Roberts, J. L., Spitzer, NC., and Zigmond, M. J. (2003) in Fundamental Neuroscience 2nd ed. pp.220, 558, and 1286–1294, Academic Press Inc., San Diego
3. Konishi, M. (1985) Annu. Rev. Neurosci. **8**, 125–170
4. Sisneros, J. A., Forlano, P. M., Deitcher, DL., and Bass, AH. (2004) Science **305**, 404–407.
5. Sisneros, J. A ., and Bass, A. H. (2003) J. Neurosci. **23**, 1049–1058
6. Bliss, T. V., and Collingridge, G. L. (1993) Nature **361**, 31–39
7. Sanes, J. R., and Lichtman, J. W. (1999) Nat. Neurosci. **2**, 597–604
8. Matsuzaki, M., Honkura, N., Ellis-Davies, G. C., and Kasai, H. (2004) Nature **429**, 761–766
9. Nagerl, U. V., Eberhorn, N., Cambridge, S. B., and Bonhoeffer, T. (2004) Neuron **44**, 759–767
10. Amaral, D. G., and Witter, M. P. (1995) Hippocampal formation, in The Rat Nervous System, second edition (Paxinos, G. ed.) pp. 443–493, Academic Press Inc., San Diego
11. Bliss, T. V., and Lomo, T. (1973) J. Physiol. **232**, 331–356
12. Bliss, T. V., and Gardner-Medwin, A. R. (1973) J. Physiol. **232**, 357–374
13. Malenka, R. C., and Nicoll, R. A. (1999) Science **285**, 1870–1874

14. Bauer, E. P., Schafe, G. E., and LeDoux, J. E. (2002) J. Neurosci. **22**, 5239–5249
15. Zalutsky, R. A., and Nicoll, R. A. (1990) Science **248**, 1619–1624
16. Johnston, D., Williams, S., Jaffe, D., and Gray, R. (1992) Annu Rev Physiol. **54**, 489–505
17. Teyler, T. J., Cavus, I., Coussens, C., DiScenna, P., Grover, L., Lee, Y. P., and Little, Z. (1994) Hippocampus. **4**, 623–634
18. Kapur, A., Yeckel, M. F., Gray, R., and Johnston, D.(1998) J. Neurophysiol. **79**, 2181–2190
19. Bashir, Z. I., Bortolotto, Z. A., Davies, C. H., Berretta, N., Irving, A. J., Seal, A. J., Henley, J. M., Jane, D. E., Watkins, J. C., and Collingridge, G. L. (1993) Nature **363**, 347–350
20. Ito, M. (2001) Physiol. Rev. **81**, 1143–1195
21. Pelkey, K. A., Topolnik, L., Lacaille, J. C., and McBain, C. J. (2006) Neuron **52**, 497–510
22. James, W. M., and Agnew, W. S. (1987) Biochem. Biophys. Res. Commun. **148**, 817–826
23. Zuber, C,. Lackie, P. M., Catterall, W. A., and Roth, J. (1992) J. Biol. Chem. **267**, 9965–9971
24. Bennett, E. S. (2002) J. Physiol. **538**, 675–690.
25. Finne. J., Finne. U., Deagostini-Bazin, H., and Goridis, C. (1983) Biochem. Biophys. Res. Commun. **112**, 482–487
26. Nakayama, J., Fukuda, M. N., Fredette, B., Ranscht, B., and Fukuda, M. (1995) Proc. Natl. Acad. Sci. USA. **92**, 7031–7035
27. Scheidegger, E. P., Sternberg, L. R., Roth, J., and Lowe, J. B. (1995) J. Biol. Chem. **270**, 22685–22688
28. Angata, K., Suzuki, M., and Fukuda, M. (2002) J. Biol. Chem. **277**, 36808–36817
29. Sadoul, R., Hirn, M., Deagostini-Bazin, H., Rougon, G., and Goridis, C. (1983) Nature **304**, 347–349
30. Rutishauser, U. (1996) Curr. Opin. Cell Biol. **8**, 679–684
31. Rutishauser, U., and Landmesser, L. (1996) Trends Neurosci. **19**, 422–427
32. Rutishauser, U. (1998) J. Cell Biochem. **70**,304–312
33. Seki, T., and Rutishauser, U. (1998) J, Neurosci. **18**, 3757–3766
34. Dityatev, A., Dityateva, G., Sytnyk, V., Delling, M., Toni, N., Nikonenko, I., Muller, D., and Schachner, M. (2004) J. Neurosci. **24**, 9372–9382
35. Fux, C. M, Krug, M., Dityatev, A., Schuster, T., and Schachner, M. (2003) Mol. Cell Neurosci. **24**, 939–950
36. Schuster, T., Krug, M., Stalder, M., Hackel, N., Gerardy-Schahn, R., and Schachner, M. (2001) J. Neurobiol. **49**, 142–158
37. Schuster, T., Krug, M., Hassan, H., and Schachner, M., (1998) J. Neurobiol. **37**, 359–372
38. Seki, T., and Arai, Y. (1999) J. Comp. Neurol. **410**, 115–125
39. Muller, D., Wang, C., Skibo, G., Toni, N., Cremer, H., Calaora, V., Rougon, G., and Kiss, J. Z. (1996) Neuron **17**, 413–422
40. Stoenica, L., Senkov, O., Gerardy-Schahn, R., Weinhold, B., Schachner, M., and Dityatev. A. (2006) Eur. J. Neurosci. **23**, 2255–2264
41. Cremer, H., Chazal, G., Carleton, A., Goridis, C., Vincent, J. D., and Lledo, P. M. (1998) Proc. Natl. Acad. Sci USA. **95**, 13242–13247
42. Angata, K., Long, J. M., Bukalo, O., Lee, W., Dityatev, A., Wynshaw-Boris, A., Schachner, M., Fukuda, M., and Marth, J. D. (2004) J. Biol. Chem. **279**, 32603–32613
43. Eckhardt, M., Bukalo, O., Chazal, G., Wang, L., Goridis, C., Schachner, M., Gerardy-Schahn, R., Cremer, H., and Dityatev, A. (2000) J. Neurosci. **20**, 5234–5244
44. Bukalo, O., Fentrop, N., Lee, AY., Salmen, B., Law, JW., Wotjak, CT., Schweizer, M., Dityatev, A., and Schachner, M. (2004) J. Neurosci. **24**, 1565–1577
45. Senkov, O., Sun, M., Weinhold, B., Gerardy-Schahn, R., Schachner, M., and Dityatev, A. (2006) J. Neurosci. **26**, 10888–109898
46. Hammond, MS., Sims, C., Parameshwaran, K., Suppiramaniam, V., Schachner, M., and Dityatev, A. (2006) J. Biol. Chem. **281**, 34859–34869
47. Hardingham, GE., Fukunaga, Y., and Bading, H. (2002) Nat. Neurosci. **5**, 405–414
48. Nakazawa, T., Komai, S., Watabe, A. M., Kiyama, Y., Fukaya, M., Arima-Yoshida, F., Horai, R., Sudo, K., Ebine, K., Delawary, M., Goto, J., Umemori, H., Tezuka, T., Iwakura, Y., Watanabe, M., Yamamoto, T., and Manabe, T. (2006) EMBO. J. **25**, 2867–2877
49. Hildebrandt H, Becker C, Murau M, Gerardy-Schahn R, and Rahmann H. (1998) J. Neurochem. **71**, 2339–2348
50. Rousselot, P., Lois, C., and Alvarez-Buylla, A., (1995) J. Comp. Neurol. **351**, 51–61
51. Tomasiewicz, H., Ono, K., Yee, D., Thompson, C., Goridis, C., Rutishauser, U., and Magnuson, T. (1993) Neuron **11**, 1163–1174
52. Chazal, G., Durbec. P., Jankovski, A., Rougon, G., and Cremer, H. (2000) J. Neurosci. **20**, 1446–1457
53. Prosser, RA., Rutishauser, U., Ungers, G., Fedorkova, L., and Glass, JD. (2003) J. Neurosci. **23**, 652–658
54. Ding, JM., Chen, D., Weber, ET., Faiman, LE., Rea, MA., and Gillette, MU. (1994) Science **266**, 1713–1717
55. Shen, H., Watanabe, M., Tomasiewicz, H., Rutishauser, U., Magnuson, T., and Glass, JD. (1997) J. Neurosci. **17**, 5221–5229
56. Theodosis, D. T., Bonhomme, R., Vitiello, S., Rougon, G., and Poulain, DA. (1999) J. Neurosci. **19**, 10228–10236
57. Hoyk, Z., Parducz, A., and Theodosis, D. T. (2001) Eur. J. Neurosci. 2001 Feb;13 (4):649–656.
58. Yoshida, K., Rutishauser, U., Crandall, J. E., and Schwarting, G. A. (1999) J. Neurosci. **19**,794–801
59. Mikkonen, M., Soininen, H., Kälviänen, R., Tapiola, T., Ylinen, A., Vapalahti, M., Paljärvi, L., and Pitkänen, A. (1998) Ann. Neurol. **44**, 923–934
60. Okabe, A., Tawara, Y., Masa, T., Oka, T., Machida, A., Tanaka, T., Matsuhashi, H., Shiosaka, S., and Kato, K. (2001) J. Neurochem. **77**,1185–1197
61. Weber M, Modemann S, Schipper P, Trauer H, Franke H, Illes P, Geiger KD, Hengstler JG, and Kleemann WJ. (2006) Neuroscience **138**, 1215–1223
62. Nguyen, L., Malgrange, B., Breuskin, I., Bettendorff, L., Moonen, G., Belachew, S., and Rigo, J. M. (2003) J. Neurosci. **23**, 3278–3294
63. Yamamoto, S., Oka, S., Inoue, M., Shimuta, M., Manabe, T., Takahashi, H., Miyamoto, M., Asano, M., Sakagami, J., Sudo, K., Iwakura, Y., Ono, K., and Kawasaki, T. (2002) J. Biol. Chem. **277**, 27227–27231
64. Senn, C., Kutsche, M., Saghatelyan, A., Bösl, MR., Löhler, J., Bartsch, U., Morellini, F., and Schachner, M. (2002) Mol. Cell Neurosci. **20**, 712–729
65. Saghatelyan, A. K., Gorissen, S., Albert, M., Hertlein, B., Schachner, M., and Dityatev, A. (2000) Eur. J. Neurosci. **12**, 3331–3342
66. Rose, S. P and Jork, R. (1987) Behav. Neural. Biol. **48**, ™246–258
67. Bullock, S., Potter, J., and Rose, SP., (1990) J. Neurochem. **54**, 135–142

68. Krug, M., Jork, R., Reymann, K., Wagner, M., and Matthies, H. (1991) Brain Res. **540**, 237–242
69. Jork, R., Smalla, K. H., Karsten, U., Grecksch, G., Rüthrich, H. L., and Matthies, H. (1991) Neurosci. Res. Commun. **8**, 21–27
70. Murrey, HE., Gama, C. I., Kalovidouris, S. A, Luo W. I., Driggers, E. M, Porton, B., and Hsieh-Wilson, L. C. (2006) Proc. Natl. Acad. Sci. USA. **103**, 21–26
71. Yamagata, M., Sanes, J.R., and Weiner, J. A. (2003) Curr. Opin. Cell Biol. **15**, 621–632
72. Rauch, U., (2004) Cell Mol. Life Sci. **61**, 2031–2045
73. Laabs, T., Carulli, D., Laabs, T., Geller, H.M., and Fawcett, J. W. (2005) Curr. Opin. Neurobiol. **15**, 116–120
74. Bukalo, O., Schachner, M., and Dityatev, A. (2001) Neuroscience. **104**, 359–369
75. Saghatelyan, AK., Dityatev, A., Schmidt, S., Schuster, T., Bartsch, U., and Schachner, M. (2001) Mol. Cell Neurosci. **17**, 226–240
76. Niisato, K., Fujikawa, A., Komai, S., Shintani, T., Watanabe, E., Sakaguchi, G., Katsuura, G., Manabe, T., and Noda, M. (2005) J. Neurosci. **25**, 1081–1088
77. Brakebusch, C., Seidenbecher, C.I., Asztely, F., Rauch, U., Matthies, H., Meyer, H., Krug, M., Böckers, T. M., Zhou, X., Kreutz, MR., Montag. D., Gundelfinger, ED., and Fässler, R. (2002) Mol. Cell Biol. **22**, 7417–7427
78. Paukert, M., and Bergles, D. E. (2006) Curr. Opin. Neurobiol. **16**, 515–521
79. Ge, W. P., Yang, X. J, Zhang, Z., Wang, H. K, Shen, W., Deng, Q. D., and Duan, S. (2006) Science **312**, 1533–1537.
80. Lauri, SE., Kaukinen, S., Kinnunen, T., Ylinen, A., Imai, S., Kaila, K., Taira, T., and Rauvala, H. (1999) J. Neurosci. **19**, 1226–1235
81. Kaksonen, M., Pavlov, I., Võikar, V., Lauri, S. E., Hienola, A., Riekki, R., Lakso, M., Taira, T., and Rauvala, H. (2002) Mol. Cell Neurosci. **21**, 158–172
82. Ishiyama, J., Saito, H., and Abe, K. (1991) Neurosci. Res. **12**, 403–411
83. Lauri, SE., Taira, T., Kaila, K., and Rauvala, H. (1996) Neuroreport **7**, 1670–1674
84. Johnson, K. G., Tenney, A. P., Ghose, A., Duckworth, A. M., Higashi, M. E, Parfitt, K., Marcu, O., Heslip, T. R., Marsh, J. L., Schwarz, T. L., Flanagan, J. G., and Vactor, DV., (2006) Neuron **49**, 517–531.
85. Johnson, K. G., and Vactor, D. V., (2003) Physiol. Rev. **83**, 1–24.
86. Everts, I., Petroski, R., Kizelsztein, P., Teichberg, V. I., Heinemann, S. F., and Hollmann, M. (1999) J. Neurosci. **19**,916–927
87. Tyrrell, L., Renganathan, M., Dib-Hajj, S. D., and Waxman, S. G., (2001) J. Neurosci. **21**, 9629–9637
88. Pasternack, A., Coleman, S. K., Féthiére, J., Madden, D. R., LeCaer, J. P., Rossier, J., Pasternack, M., and Keinanen, K. (2003) J. Neurochem. **84**, 1184–1192
89. Sallette, J., Pons, S., Devillers-Thiery, .A, Soudant, M., Carvalho, L. P., Changeux, J. P., and Corringer ,P.J. (2005) Neuron **46**, 595–607.
90. Han, W., Rhee, J. S., Maximov, A., Lao, Y., Mashimo, T., Rosenmund, C., and Südhof, T. C. (2004) Neuron **41**, 85–99
91. Furuse, H., Waki, H., Kaneko, K., Fujii, S., Miura, M., Sasaki, H., Ito, K,I., Kato, H., and Ando, S. (1998) Exp. Brain Res. **123**, 307–314.
92. Matthies, H. Jr., Kretlow, J., Matthies, H., Smalla, K. H., Staak, S, and Krug, M. (1999) Neuroscience **91**, 175–183
93. Maruo, K., Nagata, T., Yamamoto, S., Nagai, K., Yajima, Y., Maruo, S., and Nishizaki, T. (2003) Brain Res. **977**, 294–297

Received on February 18, 2007, accepted on February 20, 2007

Profile of the Author

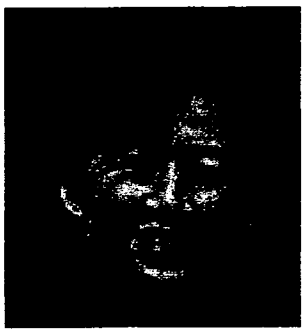

Keiko Kato is currently Associate Professor of the Graduate School of Life and Environmental Sciences, Osaka Prefecture University. She obtained D.V.M. from Osaka Prefecture University in 1987. She then graduated from Osaka University in 1987 and received her Ph.D. in biochemistry and cell biology from Osaka University in 1991. Main themes: roles of glycosylation on neural function and mechanism of epileptogenesis

Available online at www.sciencedirect.com
SCIENCE DIRECT
Cancer Letters 241 (2006) 42–48
CANCER Letters
www.elsevier.com/locate/canlet

The phototoxicity of photofrin was enhanced by PEGylated liposome in vitro

Yasuyuki Sadzuka [a,*], Koji Tokutomi [a], Fumiaki Iwasaki [a], Ikumi Sugiyama [a], Toru Hirano [b], Hiroyuki Konno [c], Naoto Oku [a], Takashi Sonobe [a]

[a] *School of Pharmaceutical Sciences, University of Shizuoka, 52-1 Yada, Shizuoka 422-8526, Japan*
[b] *Photon Medical Research Center, Hamamatsu University School of Medicine 1-20-1 Handayama, Hamamatsu, Shizuoka 431-3192, Japan*
[c] *Second Department of Surgery II, Hamamatsu University School of Medicine 1-20-1 Handayama, Hamamatsu, Shizuoka 431-3192, Japan*

Received 20 January 2005; received in revised form 8 September 2005; accepted 6 October 2005

Abstract

In recent years, photodynamic therapy (PDT) with a photosensitizer and laser has been given attention, especially for the treatment of superficial cancers, such as lung, gastric, bladder and cervical cancer. In this study, in order to enhance the efficacy of PDT, photofrin liposome (PF-Lip) was prepared with dimyristoylphosphatidylcholine, dimyristoylphosphatidylglycerol and cholesterol. Polyethyleneglycol modified photofrin liposome (PF-PEG-Lip) was prepared by modification of PF-Lip with monomethoxypolyethyleneglycol-2.3-dimyristoylglycerol. PF-Lip and PF-PEG-Lip entrapped with photofrin with 81.0 ± 5.9 and $81.2 \pm 9.2\%$, respectively. The particle size of each liposome was 114.3 ± 5.7 nm (PF-Lip) and 118 ± 3.5 nm (PF-PEG-Lip), respectively. It was suggested that PEGylated liposomes has no effect on the trapping ratio of PF and particle size. Phototoxicity was enhanced by liposomalization, especially PEG-modification. However, PF-PEG-Lip inhibited the uptake of photofrin into tumor cells. The amount of singlet oxygen from photofrin solution (PF-sol) and each liposome was PF-PEG-Lip ≒ PF-Lip > PF-sol. The photofrin release revel of PF-PEG-Lip was lower than that of PF-Lip.

In conclusion, the phototoxicity of PF-PEG-Lip was significantly higher than that of PF-sol or PF-Lip. It is expected that formation of a fixed aqueous layer on the liposome membrane by PEGylation physically changed it into the stable state of PF-PEG-Lip.

Keywords: Liposome; Photodynamic therapy (PDT); Photofrin; Singlet oxygen

1. Introduction

Photodynamic therapy (PDT), which involves photosensitizer and laser has been established as a potent and less invasive treatment for various malignant tumors [1–4]. photofrin, a hematoporphyrin derivative activated with red light of 630 nm, has been approved and commercialized in European and Asian countries, as well as in North America [5]. Especially in Japan, PDT with photofrin has been supported by government medical insurance since 1996. The antitumor effect of PDT is triggered by the singlet oxygen generated from the photosensitizer under laser irradiation [6–8].

Abbreviations PDT, photodynamic therapy; PF-Lip, photofrin liposome; PF-PEG-Lip, polyethyleneglycol modified photofrin liposome; PF-sol, photofrin solution; DMPC, L-α-dimyristoylphosphatidylcholine; DMPG, L-α-dimyristoylphosphatidyl-DL-glycerol; PEG-DMG, 1-monomethoxypolyethyleneglycol-2,3-dimyristoylglycerol; PBS, phosphate-buffered saline; T_c, transition temperature; EDL, excimer dye laser; PMT, photomultiplier tube; EPR, enhanced permeability and retention.

* Corresponding author. Tel.: +81 54 264 5610; fax: +81 54 264 5615.
E-mail address: sadzuka@u-shizuoka-ken.ac.jp (Y. Sadzuka).

0304-3835/$ - see front matter © 2005 Elsevier Ireland Ltd. All rights reserved.
doi:10.1016/j.canlet.2005.10.024

The difference in concentration of the photosensitizer makes it possible to damage tumor tissue with less damage to the surrounding normal tissues [9].

Liposomes have been applied as a carrier in various fields to modify the distribution of the chemical agents [10,11]. This strategy is based on the premise that liposomes are preferentially absorbed by sites of disease such as tumors. It is known that polyethyleneglycol (PEG)-modification of liposomes avoids trapping liposomes by the reticuloendothelial system (RES), as a result, this increases the distribution of liposomes in the tumor [12–14]. It is reported that liposomalization of the photosensitizer enhanced the effect of PDT based on its tumor accumulation [15]. Liposomal benzoporphyrin derivative monoacid ring A (BPD-MA, verteporfin) shows an enhanced therapeutic effect against Meth A sarcoma in nude mice, and liposomal 2,3-dihydro-5,15-di(3,5-dihydroxyphenyl)-porphyrin (SIM01) shows an enhanced effect against HT29 human adenocarcinoma in nude mice [16]. Furthermore, liposomal photofrin enhanced therapeutic efficacy of PDT against 9L gliosarcoma, U87 human glioma and human gastric cancer [17–19]. However, there are few reports on the phototoxicity and the effect of active oxygen generation by liposomalization of photosensitizer and its PEGylation [20].

In this study, we investigated the liposomalization of photofrin, and evaluated the cytotoxicity of liposomal photofrin in vitro with M5076 ovarian sarcoma. Furthermore, we attempted to make clear the mechanism of the enhancement of PDT through the measurement of singlet oxygen.

2. Material and method

2.1. Materials

Photofrin, porfimer sodium injection, was purchased from Nippon Lederly Co., Ltd (Tokyo, Japan). L-α-Dimyristoylphosphatidylcholine (DMPC) and L-α-dimyristoylphosphatidyl-DL-glycerol (DMPG) were kindly donated by Nippon Oil and Fat Co., Ltd (Tokyo, Japan). 1-Monomethoxypolyethylene-glycol-2,3-dimyristoylglycerol (PEG-DMG) was kindly provided by Nippon Oil and Fat Co., Ltd. RPMI-1640 medium was purchased from Nissui Pharmaceutical Co., Ltd (Tokyo, Japan).

2.2. Tumor

An M5076 ovarian sarcoma was maintained through intraperitoneal passage and implanted on the backs of male C57BL/6 mice obtained from Japan SLC, Inc. (Hamamatsu, Japan). The animals were housed in a room maintained at 25 ± 1 °C and 55 ± 5% relative humidity, and were given free access to regular food pellets and water.

2.3. Preparation of liposomes

All liposomes were prepared according to a modification of the method of Bangham et al. [21].

DMPC/cholesterol/DMPG (100/100/60 μmol) and 30 mg of photofrin were dissolved in a chloroform/-methanol mixture (4/1, v/v). The chloroform and methanol were evaporated under a stream of nitrogen gas. The thin lipid film was placed in a desiccator, which was evacuated, and then the lipid film was hydrated with 8.0 ml of phosphate-buffered saline (PBS(−)) in a water bath at 65 °C for 10 min. The suspension was sonicated for 20 min above the phase transition temperature (T_c) with nitrogen gas bubbling. The liposome suspension was extruded through two stacked polycarbonate membrane filters with 0.2 μm pores, and then passed five times through polycarbonate membrane filters with 0.1 μm pores at above the T_c, to obtain a homogeneously-sized liposome suspension. PF-Lip was prepared by adding 2.0 ml of PBS(−) to this suspension. On the other hand, PF-PEG-Lip was prepared by adding 2.0 ml of PBS(−) containing 15 μmol PEG-DMG, and then sonicated for 5 min. Each liposome suspension was dialyzed against PBS(−) at 4 °C for 16 h to remove untrapped photofrin. The particle sizes and zeta-potentials of the liposomes were measured with an electophoretic light scattering apparatus (ELS 8000; Otsuka Electronics, Co., Ltd Osaka, Japan). Entrapment efficiency of photofrin in liposome was measured to the following. Liposomes encapsulating photofrin were mixed for 30 s with lactate buffer (pH 4.0) and chloroform/isopropanol (1/1, v/v), and then centrifugated at 1200*g* for 15 min. Photofrin in the organic phase was calculated with a fluorescence spectrophotometer (Hitachi F2000; Hitachi Ltd, Tokyo), at an excitation wavelength of 405 nm and an emission wavelength of 630 nm.

2.4. PDT in vitro

M5076 ovarian sarcoma cells (1×10^5 cells/ml) were suspended in RPMI 1640 medium containing 10% FBS in a 35-mm cell culture dish. This cell suspension containing PF-sol, PF-Lip or PF-PEG-Lip (PF concentration, 2, 5 or 10 μg/ml) was incubated for 60 min at 37 °C. Each cell suspension was exposed to

laser light of 630 nm with 2 J/cm^2 of fluence (0.1 W, 192 s) and then incubated for 24 h at 37 °C. Cell survival was determined by 4-[3-(2-methoxy-4-nitrophenyl)-2-(4-nitrophenyl)-2H-5-tetrazolio]-1,3-benzene disulfonate sodium salt (WST-8) using a commercially available kit (TetraColor ONE cell proliferation assay system; Seikagaku Co., Tokyo, Japan). Each cell suspension was transferred to a microtube and centrifuged at 300*g* for 5 min. The cells were washed and resuspended in RPMI-1640 medium. TetraColor ONE (50 μl) was added to each cell suspension and incubated for 3 h at 37 °C. Each cell suspension was centrifuged at 300*g* for 5 min, and absorbances at 492 and 630 nm of the supernantant were measured using a microplate reader. Absobance (A492-A630) correlates with the number of living cells.

2.5. Uptake of photofrin into tumor cells

M5076 ovarian sarcoma cells (1×10^6 cells/animal) were intraperitonally transplanted into male C57BL/6 mice. Ascites fluid was collected on the 14th day after transplantation. The M5076 ovarian sarcoma cells were washed twice and then resuspended (5×10^6 cells/ml) in RPMI-1640 medium containing 10% FBS.

The cell suspension containing PF-sol, PF-Lip or PF-PEG-Lip (photofrin concentration, 10 μg/ml) was incubated at 37 °C for 90 min. For determination of the time course of the intracellular drug concentration, aliquots of the cell suspension were removed at intervals. Each aliquot was cooled on ice and then centrifuged at 150*g* for 3 min. The cells were washed and resuspended in 1.0 ml of ice-cold saline, mixed for 30 s with 3.0 ml THF and 0.5 g NaCl, and then centrifuged at 1200*g* for 15 min. The concentration of the photofrin in the organic phase was determined as described above.

2.6. Measurement of singlet oxygen

For the sample, PF-sol, PF-Lip, PF-PEG-Lip and photofrin were dissolved in CH_2Cl_2/EtOH (9/1, v/v). Each sample was diluted with PBS(−) or CH_2Cl_2/EtOH (9/1, v/v), in order to achieve 0.5 as the absorption at 630 nm.

A quartz cuvette filled with each sample was irradiated by laser light (630 nm, 20 mW) generated excimer dye laser (EDL). Reflected or scattered light from the cuvette was guided to the detection system (Fig. 1) which contained a spectroscope, a single channel detector PMT (Hamamatsu Photonics, R5509-42) or a multichannel detector (Hamamatsu Photonics, NIR-PII) and a photon-counter. To separate the 1270 nm emission from the photosensitizer fluorescence, detectors were gated with a delay time from the onset of the laser pulse irradiation and a gate time width, synchronized with laser the pulses. In this study, the energy generated at 1260–1280 nm was detected by the system.

2.7. Determination of the release of PF from liposomes

PF-Lip and PF-PEG-Lip were incubated in 50% FBS/PBS(−) for 3 h at 37 °C. The concentration of

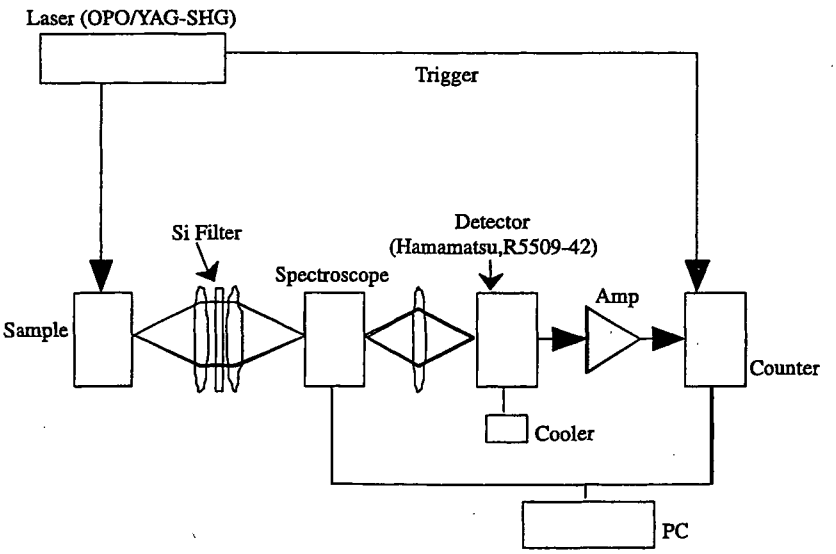

Fig. 1. Detection system of 1270 nm emission from the singlet oxygen.

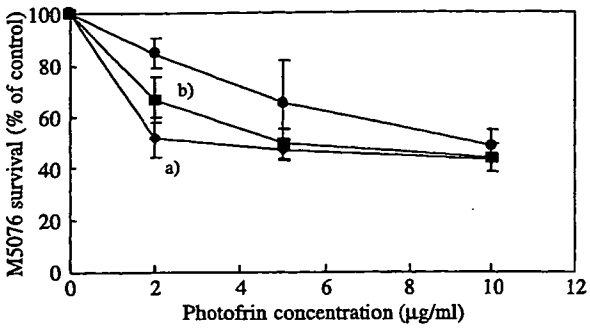

Fig. 2. Phototoxicity of photofrin against M5076 ovarian Sarcoma by PDT. M5076 ovarian sarcoma cell suspension containing PF-sol (●), PF-Lip (■) or PF-PEG-Lip (♦) (photofrin dose 2, 5 or 10 μg/ml) was incubated for 1 h at 37 °C. Each sample was exposed to laser light (630 nm, 2 J/cm^2), and was then incubated for 24 h at 37 °C. Survival ratio of M5076 ovarian sarcoma cells was determined by WST-8 assay. Data are presented as mean ± SD ($n=4$). Significant differences from PF-sol are indicated by (a) $P<0.05$ and (b) $P<0.01$.

photofrin was 1.0 μg/ml at both samples. After a predetermined time, each liposome suspension was cooled on ice and then centrifuged at 180,000*g* (4 °C) for 60 min. The photofrin concentration in the supernatant was determined as described above. The leakage of photofrin from the liposomes was calculated from the photofrin concentration in the supernantant before and after being centrifuged.

2.8. Statistical analysis

Statistical analysis was carried out by Student's *t*-test and ANOVA.

3. Results

3.1. Physicochemical characteristics of photofrin liposomes

PF-Lip and PF-PEG-Lip entrapped photofrin with 81.0 ± 5.9 and 81.2 ± 9.2% efficiency, respectively, suggesting that photofrin was stably incorporated into the lipid bilayer. The particle size of each liposome was 114.3 ± 5.7 nm (PF-Lip) and 118.4 ± 3.5 nm (PF-PEG-Lip). It was suggested that PEGylated liposomes has no effect on these particle sizes. Because of the negative charge of DMPG in the lipid bilayer, the zeta-potential of PF-Lip was −38.2 ± 9.9 mV. On the other hand, the zeta-potential of PF-PEG-Lip was −5.3 ± 9.7 mV, smaller than that of PF-Lip, since PEG formed water layer, fixed aqueous layers, on the surface of the liposomes.

3.2. PDT in vitro

M5076 ovarian sarcoma cell suspension (1.0 × 10^5 cells/ml) containing PF-sol or PF-Lip or PF-PEG-Lip was incubated for 1 h at 37 °C. Each sample was exposed to laser light of 630 nm with 2 J/cm^2. At every concentration, the photofrin induced cytotoxic effect was PF-sol < PF-Lip < PF-PEG-Lip, suggesting that photosensitizer induced toxicity was enhanced by liposomalization, especially PEGylation. At the point of 2 μg/ml photofrin, survival ratios in PF-Lip and PF-PEG-Lip group significantly decreased ($P<0.05$ and $P<0.01$, respectively), compared to that in PF-sol group (Fig. 2).

3.3. Uptake of photofrin into tumor cells

In the determined period, the intercellular photofrin level was PF-Lip > PF-sol > PF-PEG-Lip. Especially at 60 min, a significant difference ($P<0.01$) was observed (Fig. 3, PF-Lip: 2.45 ± 0.31, PF-sol: 1.20 ± 0.11, PF-PEG-Lip: 0.61 ± 0.04 μg/10^7 cells).

3.4. Measurement of singlet oxygen

A laser beam of 630 nm and 20 mW irradiated PF-sol, PF-Lip, PF-PEG-Lip and photofrin in 90% CH_2Cl_2. Then, the emission at 1260–1280 nm was detected by the system, and accumulated these photon counts. As a result, it was suggested that the amount of singlet oxygen generated by irradiation was PF-PEG-Lip ≒ PF-Lip > PF-sol (Fig. 4, Table 1). Futhermore, photofrin in 90% CH_2Cl_2 generated more singlet oxygen than PF-PEG-Lip. There were reproducibility about this results.

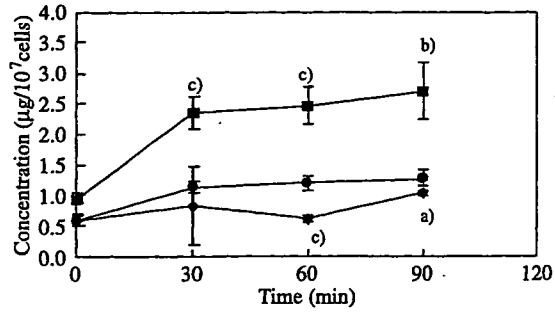

Fig. 3. Effect of liposomalization on photofrin uptake in M5076 ovarian sarcoma. Tumor cell suspension containing PF-sol (●), PF-Lip (■) or PF-PEG-Lip (♦) (photofrin dose 10 mg/kg) was incubated at 37 °C. Data are presented as mean ± SD ($n=4$). Significant differences from PF-sol are indicated by (a) $P<0.05$, (b) $P<0.01$ and (c) $P<0.005$.

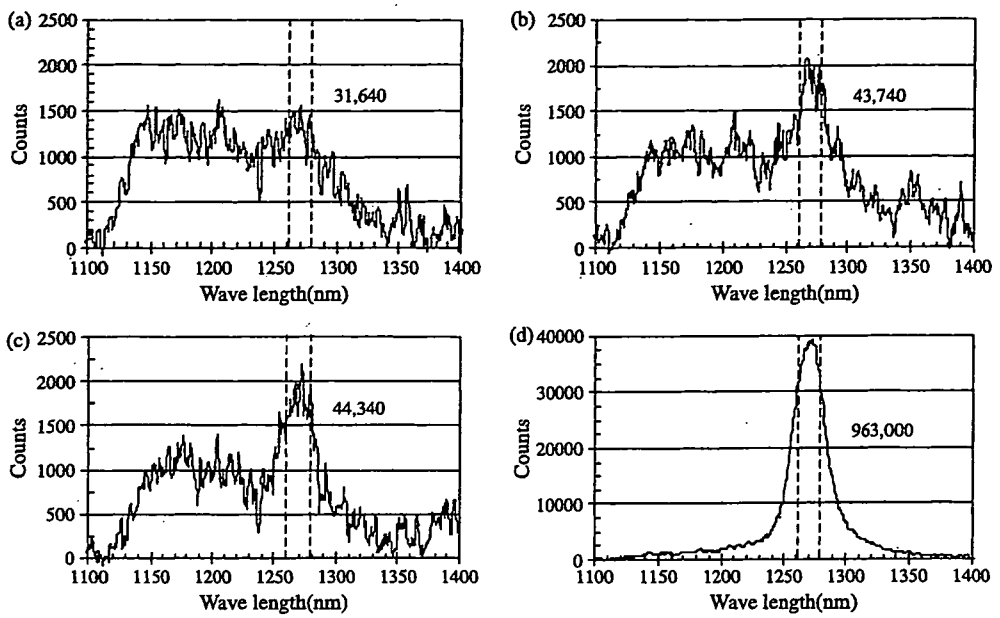

Fig. 4. Emission of 1270 nm from photofrin. Each sample was exposed to laser light (630 nm, 20 mW), and the generated singlet oxygen was detected by PMT. (A) Photofrin in PBS, (B) PF-Lip in PBS, (C) PF-PEG-Lip in PBS, (D) photofrin in 90% CH_2Cl_2.

3.5. Determinaton of the release of photofrin from liposomes

The photofrin release from each liposome was examined by incubation at 37 °C in 50% FBS/-PBS(−). At the initial 60 min, 79.6±5.4% of photofrin was released from PF-Lip; the remainder was released by 180 min (Fig. 5). On the other hand, only 60.6± 16.3% of photofrin was released by PF-PEG-Lip (Fig. 5). It was suggested that the release of photofrin was inhibited by PEG-modification.

4. Discussion

PDT has been considered to show favorably in the treatment of malignant tumors since both novel photosensitizers and laser systems have developed recently, and further development can be expected in the future. The cytotoxicity of PDT is caused by the photochemical reaction that occurs when the photosensitizer is exposed to the light of a specific wavelength. Several reports have demonstrated that liposomalization of the photosensitizer enhanced the efficiency of PDT based on high accumulation in the tumor [22–26]. We previously reported that liposomal photofrin enhanced therapeutic efficacy of photodynamic therapy. Furthermore, the phototoxicity and the effect of active oxygen generation by liposomalization of AlPcS4 and its PEGylation have been reported [27]. However, in the case of photofrin as clinical medicine, the improvement of therapeutic index are not examined sufficiently. Thus, we examined the usefulness of liposome as a drug carrier and other function.

Generally, it is considered that a lower trapped ratio is shown in case of liposomalization of the hydrophilic agent by the method of Bangham, since the volume proportion of the inner/outer compartment is very small when it is entrapped in the inner compartment. As photofrin is an acidic drug (pKa≒5.8) and PBS(−) (pH 7.0) are used for hydration, the rate of the ionized form is about 94.1%, so photofrin is easily entrapped in inner compartment of the liposome. However, since the photofrin trapping ratio in both PF-Lip and PF-PEG-Lip was more than 80%, it was expected that photofrin was entrapped in the liposome membrane, too. Namely, it was suggested that photofrin existed in the liposome membrane and inner compartment.

Table 1
Generation ability of the singlet oxygen

	Absorption	Area under the photon count curve	Ratio
PF-sol	0.5	31,640	1.00
PF-Lip	0.5	43,740	1.38
PF-PEG-Lip	0.5	44,340	1.40
PF-in CH_2Cl_2	0.5	963,000	30.4

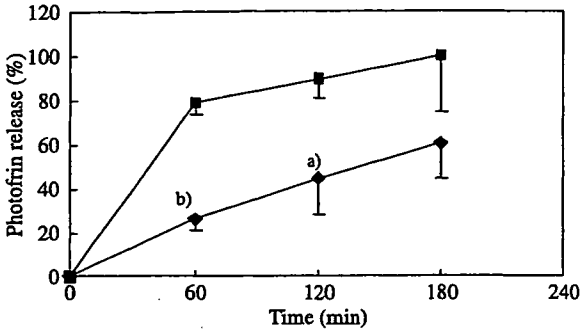

Fig. 5. Stability of liposomes containing photofrin. Photofrin release levels are expressed as a percentage of total photofrin in PF-Lip (■) or PF-PEG-Lip (♦). Each sample was incubated at 37 °C in 50% FBS. Data are presented as mean ± SD ($n=3$). Significant differences from PF-sol are indicated by (a) $P<0.01$ and (b) $P<0.001$.

We evaluated the survival ratio of M5076 ovarian sarcoma after PDT with PF-sol or each photofrin liposome. The survival of M5076 ovarian sarcoma was PF-sol > PF-Lip > PF-PEG-Lip (Fig. 2) and there were significant differences between each group. In contraction, on photofrin induced adverse reaction, we previously reported that dark toxicity of the formation used was not observed [28]. These results suggested that the phototoxicity of the photosensitizer was enhanced by liposomalization, especially by PEGylation.

Then, in order to clarify the enhanced effect of the PEGylation, we investigated the uptake of photofrin into tumor cells, ability to generate the singlet oxygen and the release of photofrin from the liposome. We evaluated the effect of liposomalization of photofrin on the uptake into M5076 ovarian sarcoma cells. As a result, the concentration of intracellular photofrin was the highest in PF-Lip group, whereas that of PF-PEG-Lip was lower than PF-sol (Fig. 3). These results suggested that the layer of PEG existed on the surface of the liposome membrane inhibits the binding of liposomes to cells, and thus prevents internalization of liposomes into the cells.

The photosensitizer loaded into the tumor cells generates singlet oxygen by laser irradiation, and thus necrosis is induced in the cells [5–8]. Namely, it is expected that the affinity of agent to tumor cell, and the ability to generate singlet oxygen is the most important factor of PDT therapy [7].

It is considered that the cytotoxicity of PDT is triggered by the singlet oxygen generated from the photosensitizer [6–8], and detection of the singlet oxygen is very important in understanding the mechanism of PDT. We measured the amount of singlet oxygen from PF-sol, PF-Lip, PF-PEG-Lip and PF in 90% CH_2Cl_2 in comparison to photofrin in aqueous solvent. On exposure to light of a specific wavelength, the photosensitizer is activated from its ground state S_0 to the excited state S_1. A part of the photosensitizer in the S_1 state transfers to the triplet state T_1 by way of intersystem crossing, and then the photosensitizer in the T_1 state transfers its energy to surrounding triplet oxygen ($^3O_2$), and causes the generation of active singlet oxygen ($^1O_2$). When the singlet oxygen decays to the triplet state, 1270 nm light is released. We detected this emission using a photon-counting method with a high sensitive single channel detector, photomultiplier tube (PMT) or a multichannel detector. The amount of singlet oxygen from photofrin was PF-PEG-Lip ≒ PF-Lip > PF-sol. It is known that singlet oxygen disappears immediately in aqueous solvents such as PBS(−), and their $T_{1/2}$ is prolonged in hydrophobic solvents such as CH_2Cl_2. It is known that singlet oxygen in aquenous solvents disappears rapidly. photofrin existed in liposome membrane as hydrophobic environment and the ability to generate singlet oxygen increased. It was suggested that the ability to generate singlet oxygen was influenced in the PDT by liposomalization and the PEGylated liposome.

The photofrin release from each liposome was PF-Lip > PF-PEG-Lip in 50%FBS/PBS(−) (Fig. 5). In particular, in PF-Lip, photofrin was released from the liposome during the incubation period. Since phase transition temperature of DMPC is 23 °C, PF-Lip may easily release photofrin by incubation at 37 °C. These results suggested that photofrin entrapped in the liposome membrane was not stable. Whereas, the PEGylated liposome inhibited the release of photofrin by about half. It was considered that formation of a fixed aqueous layer on the liposome membrane by PEGylation physically changed it into the stable state of PF-PEG-Lip. Due to this change, PF-PEG-Lip prolonged the photofrin retention time in its membrane. Namely, it was demonstrated that PF-PEG-Lip was effective for PDT in vitro.

Many previous reports have suggested that liposomalization of agents increases its accumulation in the tumor because of enhanced permeability and retention (EPR) effects [22–26]. Furthermore, it was known that the PEGylation was effective for the avoidance of RES trapping of liposomes. Therefore, PF-PEG-Lip is expected to produce a higher accumulation in the tumor than PF-Lip, and have a superior PDT effect in vivo, too.

In this study, we found the novel superiority of liposomalization on addition of function as the drug carrier in PDT. PEGylation of the liposomes prolonged

the retention time of the photosensitizer in the liposome membrane, thus showing significantly higher cytotoxicity. It is considered that this will make a great contribution to study of PDT.

References

[1] T. Hirano, The present condition of the laser for PDT, J. Jpn. Soc. Laser Surg. Med. 21 (2000) 129–135.

[2] K. Itou, T. Kano, S. Kobayashi, The photodynamic therapy over endoscope-early stomach cancer, Biotherapy 5 (1991) 546–551.

[3] H. Kato, H. Takahasi, T. Konaka, M. Ishii, T. Miura, The photodynamic therapy of lung cancer, Biotherapy 5 (1991) 536–545.

[4] H. Hisazumi, The photodynamic therapy in a urology department domain, J. Jpn. Soc. Laser Surg. Med. 8 (1987) 11–14.

[5] Wesley.M. Sharman, Cynthia.M. Allen, Johan.E. Van Lier, Photodynamic therapeutics: basic principles and clinical applications, Drug Discov. Today 4 (11) (1999) 507–717.

[6] Y.N. Konan, R. Gurny, E. Allemann, State of the art in the delivery of photosensitizers for photodynamic therapy, Photochem. Photobiol. 66 (2002) 89–106.

[7] M.C. DeRosa, R.J. Crutchley, Photosensitized singlet oxygen and its applications, Coord. Chem. Rev. 233–234 (2002) 351–371.

[8] R.D. Almeida, B.J. Manadas, A.P. Carvalho, C.B. Duarte, Intracellular signaling mechanisms in photodynamic therapy, Biochim. Biophys. Acta 1704 (2004) 59–86.

[9] D.A. Bellnier, T.J.A. Dougherty, Preliminary pharmacokinetic study of intravenous photofrin in patients, J. Clin. Laser Med. Surg. 14 (1996) 311–314.

[10] Y.M. Rustem, C. Dave, E. Mayhew, D. Papahadjopoulos, Role of liposome type and ruote of administration in the antitumor activity of liposome-entrapped 1-bate-D-arabinofuranosylcytosine against mouse L1210 Leukemia, Cancer Res. 39 (1979) 1390–1395.

[11] R.M. Abra, C.A. Hunt, D.T. Lau, Liposome disposition in vivo, J. Pharm. Sci. 73 (1984) 203–206.

[12] T. Yuda, Y. Pongpaibul, K. Maruyama, M. Iwatatsuru, Activity of amphipathic polyethylene glycol prolong the circulation time of liposomes, J. Pharm. Sci. Jpn 59 (1999) 32–42.

[13] A. Gobizon, D. Goren, A.T. Horowitz, D. Tzemach, A. Lossos, T. Siegal, Long-circulating liposomes for drug delivery in cancer therapy: a review of biodistribution studies in tumor-bearing animals, Adv. Drug Deliv. Rev. 24 (1997) 337–344.

[14] Y. Sadzuka, S. Nakai, A. Miyagishima, Y. Nozawa, S. Hirota, The effect of dose on the distribution of adriamycin encapsulated in polyethyleneglycol-coated liposomes, J. Drug Target. 3 (1995) 31–37.

[15] A.S. Derycke, P.A. de Witte, Liposomes for photodynamic therapy, Adv. Drug Deliv. Rev. 56 (2004) 17–30.

[16] B. Ludovic, T. Sonia, F. Monica, F. Yann, S. Gerard, P. Thierry, In vivo photosensitizing efficiency of a diphenylchlorin sensitizer: interest of a DMPC liposome formulation, Pharm. Res. 47 (2003) 253–261.

[17] F. Jiang, L. Lilge, B. Logie, Y. Li, M. Chopp, Photodynamic therapy of 9L gliosarcoma with liposome-delivered photofrin, Photochem. Photobiol. 65 (1997) 701–706.

[18] F. Jiang, L. Lilge, J. Grenier, Y. Li, M.D. Wilson, M. Chopp, Photodynamic therapy of U87 human glioma in nude rat using liposome-delivered photofrin, Laser Surg. Med. 22 (1998) 74–80.

[19] A. Igarashi, H. Konno, T. Tanaka, S. Nakamura, Y. Sadzuka, T. Hirano, et al., Liposomal photofrin enhances therapeutic efficacy of photodynamic therapy against the human gastric cancer, Toxicol. Lett. 145 (2003) 133–141.

[20] E. Gross, B. Ehrenberg, F.M. Johnson, Singlet oxygen generation by porphyrins and the kinetics of 9,10-dimethylanthracene photosensitization in liposomes, Photochem. Photobiol. 57 (1993) 808–813.

[21] A.D. Bangham, M.M. Standish, J.C. Watlcins, Diffusion of univalent ion across the lamellae of swollen phospholipids, J. Mol. Biol. 13 (1965) 238–252.

[22] G.C. Lin, M.L. Tsoukas, M.S. Lee, S. Gonzalez, G. Vibhagool, R.R. Anderson, et al., Skin necrosis due to photodynamic action of benzoporphyrin depends on circulating rather than tissue drug levels: implications for control of photodynamic therapy, Photochem. Photobiol. 68 (1998) 575–583.

[23] Wong Zhi-Jin, He Yu-Ying, Huang Chao-Guo, Huang Jin-Sheng, Huang Ying-Sheng, Huang Ying-Cai, et al., Pharmacokinetics, tissue distribution and photodynamic therapy efficacy of liposomal-delivered Hypocrellin A, a potential photosensitizer for tumor therapy, Photochem. Photobiol. 70 (1999) 773–780.

[24] M.H. Reinke, C. Canakis, D. Husain, N. Michaud, T.J. Flotte, E.S. Gragoudas, et al., Verteporfirin photodynsmic therapy reteament of nomal retina and choroids in the cynomolgus monkey, Ophthalmology 106 (1999) 1915–1923.

[25] A.V. Reshetnikov, I.V. Zhigaltsev, S.N. Kolomeichuk, A.P. Kaplun, V.I. Shvets, O.S. Zhukava, et al., Preparation and certain properties of the liposomal substance 2,4-di(1-methyl-3-hydroxybutyl)- deuterporphyrin-IX, Bioorg. Khim. 25 (10) (1999) 782–790.

[26] L. Lile, B.C. Wilson, Photodynamic therapy of intracranial tissues: a preclinical comparative study of four different photosensitizers, J. Clin. Laser Med. Surg. 16 (1998) 81–91.

[27] A. Gijsens, A. Derycke, L. Missiaen, D.D. Vos, J. Huwyler, A. Eberle, et al., Targeting of the photocytotoxic compound AlPcS4 to hela cells by transferring conjugated PEG-liposomes, Int. J. Cancer 101 (2002) 78–85.

[28] H. Konno, A. Igarashi, T. Tanaka, S. Nakamura, Y. Sadzuka, T. Hirano, et al., Liposomal photofrin enhances therapeutic efficacy of photodynamic therapy against the human gastric cancer, 93th AACR, Abstracts, 2002, p. 651.

Available online at www.sciencedirect.com
ScienceDirect
Journal of Controlled Release 118 (2007) 303–309
journal of controlled release
www.elsevier.com/locate/jconrel

Effective tumor regression by anti-neovascular therapy in hypovascular orthotopic pancreatic tumor model

Sei Yonezawa, Tomohiro Asai, Naoto Oku *

Department of Medical Biochemistry and COE Program in the 21st Century, University of Shizuoka School of Pharmaceutical Sciences, 52-1 Yada, Suruga-ku, Shizuoka 422-8526, Japan

Received 10 September 2006; accepted 21 December 2006
Available online 5 January 2007

Abstract

Pancreatic cancer is one of the most serious cancers with poor therapeutic results and prognosis. In here, we proposed a novel treatment strategy of pancreatic cancer by injuring limited angiogenic vessels with liposome containing adriamycin. At first, we established an orthotopic tumor model, which has a hypovascular characteristic of pancreatic tumor. In this model, we obtained the enhanced therapeutic efficacy with liposome that modified by polyethylene glycol (PEG) and a peptide, Ala-Pro-Arg-Pro-Gly (APRPG), having an affinity to neovessels. Histochemical analysis suggested the degradation of angiogenic vessels after treatment with APRPG-PEG-liposomal adriamycin. In addition, we observed colocalization of fluorescence-labeled APRPG-PEG-liposome with angiogenic endothelial cells, although the biodistribution of ^{3}H-labeled liposome did not show the difference in the amount of accumulation between PEG-modified liposome and APRPG-PEG-modified liposome. These results suggested the availability of the anti-neovascular therapy against pancreatic cancer and supply a new sight indication on chemotherapeutics against pancreatic cancer.

Keywords: Anti-neovascular therapy; Liposome; Pancreatic cancer; Angiogenesis

1. Introduction

Pancreatic cancer is one of the most difficult cancers to control: This cancer is difficult to diagnose, and shows high malignant potential. Five-year survival of patients suffering pancreatic cancer is less than 5% in the United States, Japan and Europe, and the incidence rate of it is equal to the death rate [1]. Therefore, it is suggested that existing chemotherapeutics have a limitation of the effect on pancreatic cancer, and an effective treatment modality is awaited. It is interesting to note that pancreatic cancer has less vasculature in number than other cancers such as breast or colorectal cancer known as vasculature-rich cancers. In computed tomography (CT) and magnetic resonance imaging (MRI), pancreatic tumor is considered as a hypovascular lesion compared to normal pancreatic tissue [2–4]. This property can be thought as the reason why effective pancreatic tumor chemotherapy cannot be expected due to the low bioavailability of the chemotherapeutic drugs.

On the other hand, angiogenic vessels are known to play an important role in pancreatic tumor progression as well as other tumors [5]. In general, anti-angiogenic therapy is thought to be effective for cancer treatment. Actually, many anti-angiogenic therapies that inhibit the certain steps of angiogenesis have examined. For example, matrix metalloproteinase inhibitors and anti-vascular endothelial growth factor (VEGF) agents etc., have been developed [6–8]. However, they are thought to be limited for the induction of tumor dormancy [9,10]. We previously proposed a novel therapeutic strategy targeted angiogenic vessels, cancer anti-neovascular therapy (ANET), that kills the proliferative endothelial cells followed by indirect induction of tumor regression [11,12]. Neovessel endothelial cells are growing, so it can be thought that these cells are susceptible to anti-cancer drugs like tumor cells. The benefits that can be gained from ANET are not only the effective tumor treatment but also the inhibition of tumor hematogenous metastasis, the avoidance of drug resistance, and wide range of application

* Corresponding author. Tel.: +81 54 264 5701; fax: +81 54 264 5705.
E-mail address: oku@u-shizuoka-ken.ac.jp (N. Oku).

0168-3659/$ - see front matter © 2007 Elsevier B.V. All rights reserved.
doi:10.1016/j.jconrel.2006.12.024

against many kinds of tumors. For ANET, we previously isolated APRPG peptide from a phage-displayed peptide library by biopanning of phage clones specifically bound to tumor angiogenic vasculature. *In vitro* study, we observed higher uptake of APRPG-modified liposome in human umbilical vein endothelial cells (HUVECs) than non-modified one. Furthermore, higher accumulation of APRPG-modified liposomes in tumor tissue than non-modified one was also observed in tumor-bearing mice [12].

In here, we carried out a series of experiments focused on the application of ANET to pancreatic tumor model, since it is thought that ANET is more effective in hypovascular tumors than hypervascular tumors. Firstly, we established hypovascular orthotopic pancreatic tumor model, following the investigation of biodistribution of angiogenic vessel-targeted liposome in the tumor-bearing mice. In this experiment, we used APRPG-polyethyleneglycol (PEG)-modified liposome as the angiogenic vessel-targeted liposome. Modification by PEG is known to protect liposomes from opsonization and contact with lipoproteins through the formation of aqueous layers on the surface of liposomes. Thus, the APRPG-PEG-modified liposome could have long-circulating characteristic, and would have more chance to contact with neovasculature. Next, we examined the intratumoral distribution of liposomes by using confocal laser scan microscopy. And finally, we treated the orthotopic pancreatic tumor model with APRPG-PEG-modified liposomes encapsulating adriamycin (ADM) and evaluated the therapeutic effect. The obtained data indicated that ANET is effective for pancreatic tumor treatment.

2. Materials and methods

2.1. Materials

Distearoylphosphatidylcholine (DSPC) and distearoylphosphatidylethanolamine (DSPE) were kindly gifted form Nippon Fine Chemical Co., Ltd. (Hyogo, Japan). PEG-APRPG-conjugated DSPE (DSPE-PEG-APRPG) and PEG-conjugated DSPE (DSPE-PEG) were prepared as described previously [13]. Cholesterol was purchased from Sigma (St. Louis, MO, USA). All other reagents used were the analytical grades.

2.2. Cell culture

Human pancreatic cancer cell line SUIT-2 was generously donated by Dr. Haruo Iguchi (National Kyushu Cancer Center, Fukuoka, Japan). SUIT-2 cells were cultured in RPMI 1640 supplemented with streptomycin, penicillin, and 10% fetal bovine serum (FBS, Sigma) at 37 °C in a humidified atmosphere containing 5% CO_2.

2.3. Orthotopic tumor model

BALB/c nude mice were anesthetized by intraperitoneal injection of pentobarbital (Dainippon Sumitomo Pharmaceutical Co., Ltd. Osaka, Japan). After cutting abdomen of a mouse, pancreas was exteriorized and dilated on its belly sterilized by chlorhexidine gluconate solution. Then 20 μL of SUIT-2 cells (5×10^6 cells/mouse) were injected into pancreas. Then cut area was sutured and sterilized by chlorhexidine gluconate solution.

2.4. Histopathological examination

SUIT-2 cells (5×10^6 cells/mouse) were inoculated as described in the Section 2.3. At day 3 and 9 after tumor implantation, mice were sacrificed and tumor was dissected. The tumor was embedded in optimal cutting temperature compound (Sakura Finetechnochemical Co., Ltd., Tokyo, Japan) and frozen at −80 °C. Nine-micrometer tumor sections were prepared by using cryostatic microtome (HM 505E, Microm, Walldorf, Germany), mounted on MAS coated slides (Matsunami Glass Ind., Ltd., Japan), and air-dried for 1 h. The tumor tissue sections prepared were stained with hematoxylin-eosin and histopathological examination was performed.

2.5. Evaluation of micro vessel density (MVD) in pancreatic tumor model

SUIT-2 cells (5×10^6 cells/mouse) were inoculated as described in the Section 2.3. On the day 10 and 25 after tumor implantation, mice were sacrificed and the tumor section was prepared as described in the Section 2.4. The tumor tissue sections prepared were fixed in acetone for 10 min at room temperature, washed twice with phosphate-buffered saline (PBS), pH 7.4, (5 min each time), and incubated with protein-blocking solution containing 1% bovine serum albumin in PBS for 10 min at room temperature. Then, the samples were incubated with an appropriately diluted (1:50) biotinylated anti-mouse CD31 rat monoclonal antibody (Becton Dickinson Lab., Franklin Lakes, NJ, USA) for 18 h at 4 °C. After the sections were rinsed thrice (2 min each time) with PBS, they were incubated with streptavidin-Alexa fluor® 488 conjugates (Molecular Probes Inc., Eugene, OR, USA) for 30 min at room temperature in a humid chamber. Samples were washed twice with PBS (2 min each time). Finally, sections were counterstained and mounted with Perma Fluor Aqueous Mounting Medium (Thermo Shandon, Pittsburgh, PA, USA). These sections were fluorescently observed by using microscopic LSM system (Carl Zeiss, Co., Ltd.): Endothelial cells were identified as green fluorescence. Hot spot area of the samples and CD31 positive area were quantified by ImageJ software to obtain micro vessel density (MVD). For immunostaining, the sections treated with biotinylated anti-mouse CD31 rat monoclonal antibody were stained with VECTASTAIN® ABC Kit (Vector Laboratories, Inc., Burlingame, CA, USA) by using diaminobenzidine tetrahydrochloride (DAB, Funakoshi Co., Ltd., Tokyo, Japan) as a colorimetric substrate. Then the sections were rinsed with PBS and co-stained with hematoxylin.

2.6. Preparation of liposomes

Liposomes composed of DSPC and cholesterol with DSPE-PEG or DSPE-PEG-APRPG (10:5:1 as a molar ratio, PEG-Lip and APRPG-PEG-Lip, respectively) were prepared as described

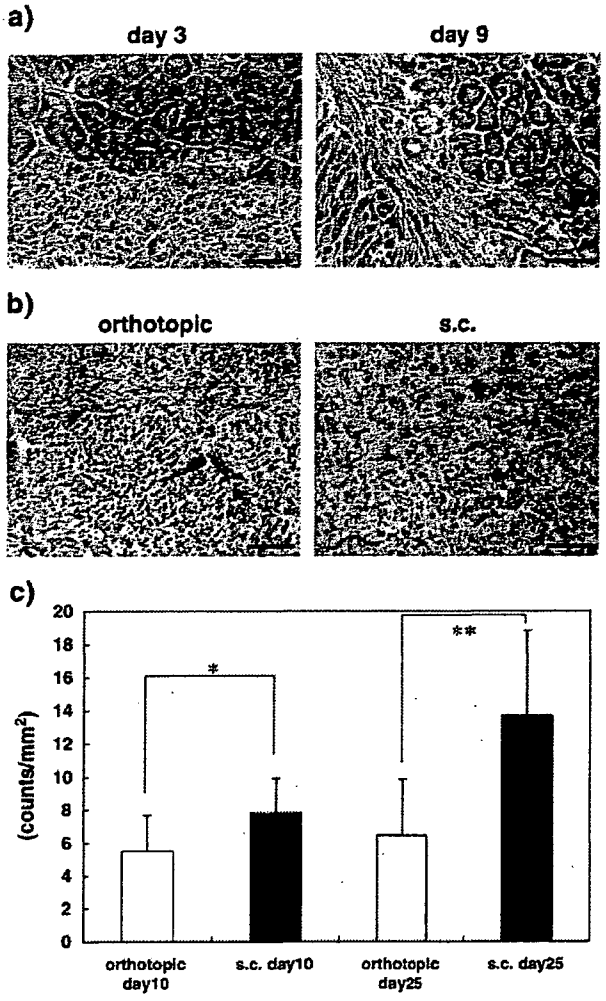

Fig. 1. Characteristics of orthotopic pancreatic tumor model. SUIT-2 cells (5×10^6 cells) were implanted into the pancreas of BALB/c nude mice. At day 3 and 9 after the tumor implantation, mice were sacrificed and tumor sections were prepared as described in Materials and methods. Then they were stained with hematoxylin and eosin (a). On the day 10 and 25, tumor sections were also prepared for evaluating vasuclarization. The sections were immunostained with biotinylated anti-mouse CD31 monoclonal antibody, and visualized with DAB as colorimetric substarate (b) or streptavidin-Alexa fluor® 488 conjugated-second antibody. CD31 positive area was observed fluorescently by a laser scanning microscopy and was quantified by ImageJ software (c). Significant differences are shown with asterisks: *, $p<0.05$ and **, $p<0.01$. Scale bar represents 100 μm.

previously [14]. In brief, lipids were dissolved in chloroform or chloroform/methanol, dried under reduced pressure, and stored *in vacuo* for at least 1 h. Then, the liposomes were formed by hydration of the thin lipid film with 0.3 M glucose, and frozen and thawed for 3 cycles using liquid nitrogen. Then liposomes were sized by thrice extrusion through a polycarbonate membrane filter with 100-nm pores. For a biodistribution study, a trace amount of [^{3}H]-cholesterylhexadecylether (Amersham Pharmacia, Buckinghamshire, UK) was added to the initial chloroform/methanol solution as described above. To observe the intratumoral distribution of liposomes, they were fluorescently labeled with 1,1′-dioctadecyl-3, 3, 3′, 3′-tetramethylindocarbocyanine perchlorate (DiI C_{18}; Molecular Probes Inc., Eugene, OR, USA), which was added to them at the quantity equivalent to 1 mol% of DSPC. For therapeutic experiment, ADM-encapsulated liposome was prepared by a modification of the remote-loading method as described previously [14]. The concentration of ADM was determined at 484 nm absorbance.

2.7. Biodistribution of liposome

Biodistribution study was performed at day 10 after SUIT-2 tumor implantation. Orthotopic pancreatic tumor model mice were injected with radiolabeled liposomes containing [^{3}H] cholesterylhexadecylether *via* a tail vein. Three or twenty-four hours after injection, the mice were sacrificed under diethyl ether anesthesia for the collection of the blood. Then the blood was centrifuged (600 ×*g* for 5 min) to obtain the plasma. After the mice had been bled from the carotid artery, the heart, lung, liver, spleen, kidney and tumor were removed, washed with saline and weighed. The radioactivity in each organ as well as plasma was determined with a liquid scintillation counter (Aloka LSC-3100). Distribution data are presented as % dose per 100-mg wet tissue, where the total amount in plasma was calculated based on the average mice body weight, which was 25.5 g and average plasma volume, which was assumed to be 4.27% of body weight based on the data of total blood volume. The animals were cared for according to the animal facility guidelines of the University of Shizuoka.

2.8. Intratumoral distribution of liposome

DiI C_{18}-labeled liposomes were administered *via* a tail vein of mice with orthotopic pancreatic tumor on the day 3, 9 and 18

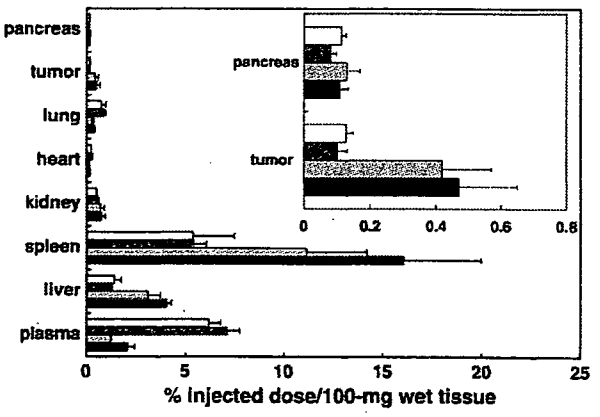

Fig. 2. Biodistribution of ^{3}H-labeled liposomes in various organs. Orthotopic pancreatic tumor model mice were injected with ^{3}H-labeled-PEG-modified liposome or APRPG-PEG-modified liposome *via* a tail vein at day 10 after tumor implantation. Three and twenty-four hours after injection, mice were dissected and the radioactivity in each organ was determined ($n=3$). Data are presented as percent of the injected dose per 100 mg tissue and S.D. Inset indicates the liposomal accumulation in the tumor and in pancreas represented as the percent-injected dose per 100 mg wet tissue. Data represents 3 h PEG-Lip (open bar), 3 h APRPG-PEG-Lip (dark gray bar), 24 h PEG-Lip (light gray bar) and 24 h APRPG-PEG-Lip (closed bar), respectively.

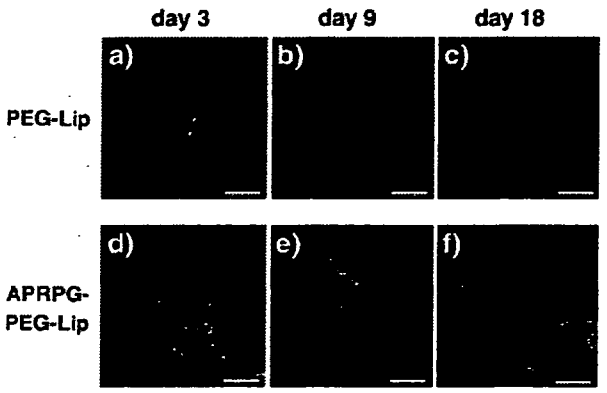

Fig. 3. Intratumoral distribution of $DiIC_{18}$-labeled liposomes. Orthotopic pancreatic tumor model mice were injected with PEG-Lip (a–c) or APRPG-PEG-Lip (d–f) labeled with $DiIC_{18}$ *via* a tail vein at day 3 (a, d), day 9 (b, e), and day 18 (c, f) after tumor implantation. At 2 h after injection of fluorescence-labeled liposomes, frozen-sections of each tumor were prepared. Green portions indicate CD31-positive regions, red portions liposomal distribution, and yellow portions show the localization of liposomes at the site of vascular endothelial cells. Scale bar represents 50 μm.

after tumor implantation. Two hours after injection of liposomes, mice were sacrificed under diethyl ether anesthesia and the tumor was dissected. Preparation of tumor sections and CD31 staining were performed as described in the Section 2.5. These tumor sections were fluorescently observed by using microscopic LSM system (Carl Zeiss, Co., Ltd.): Endothelial cells were identified as green fluorescence and liposomes were detected as red.

2.9. Therapeutic experiment

Orthotopic pancreatic tumor model was prepared by the injection of SUIT-2 cells (5×10^6 cells/mouse). Liposomes encapsulating ADM or 0.3 M glucose solution were administered intravenously into SUIT-2-bearing mice at day 3, 6, 9 and 12 after the tumor cell implantation. The injected dose of liposomal ADM in each administration was 10 mg/kg as ADM. The weight of tumor was examined at day 15. For histochemical analysis, the sections of tumor were prepared, and then immunostaining with anti-CD31 antibody and hematoxylin-eosin staining were performed as described above.

2.10. Statistical analysis

Student's *t*-test was used for statistical analysis, and $p<0.05$ were considered to be statistically significant.

3. Results

3.1. Preparation of orthotopic pancreatic tumor model

At first, we examined the characteristics of orthotopic pancreatic tumor model by using SUIT-2 human pancreatic tumor cell line. Histopathological examination indicated that tumor cells invaded into neighboring pancreatic tissue at 3 and 9 days after tumor implantation (Fig. 1a). Then we investigated whether the model showed hypovascular characteristics or not. For this purpose, vascular density of the model was compared with that of s.c. implanted SUIT-2 tumor model. The result of immunostaining with anti-CD31 antibody showed that MVD of orthotopic pancreatic tumor model was lower than that of s.c. implanted model (Fig. 1b): The significant differences were observed in CD31 positive area of day 10-orthotopic model mice from that of day 10-s.c. model mice ($p<0.05$), day 25-orthotopic model mice from day 25-s.c. model mice ($p<0.01$). These data indicated that orthotopic implantation of SUIT-2 cells developed pancreatic tumor with hypovascular characteristics. The immunostaining study also confirmed the hypovascular characteristics of the orthotopic pancreatic tumor model (Fig. 1c).

3.2. Biodistribution of liposomes

Before therapeutic experiment, we investigated the biodistribution of the liposome in the orthotopic pancreatic tumor-bearing mice, since the accumulation of drug carrier is prerequisite for the therapeutic effect of entrapped drugs in the carrier at the target site. Ten days after SUIT-2 tumor implantation, ^{3}H-labeled PEG-Lip or APRPG-PEG-Lip was injected *via* a tail vein. Three and twenty-four hours after injection of liposomes, mice were sacrificed and tumor and other organs were dissected for measuring the radioactivity in these tissues. Both PEG-Lip and APRPG-PEG-Lip accumulated in tumor time-dependently, although there was no significant difference between those two kinds of liposomes (Fig. 2). Therefore, even though in the hypovascular tumor, enhanced permeability and retention (EPR) effect of liposomes is achieved to some extent.

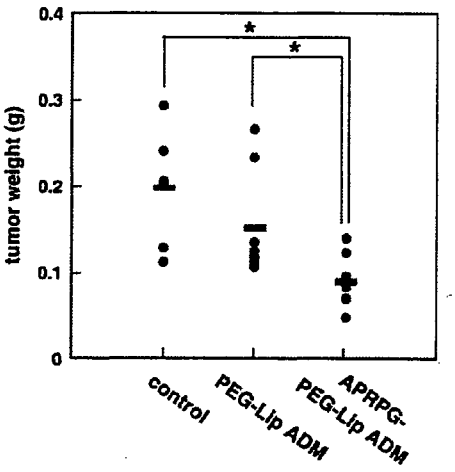

Fig. 4. Therapeutic effect of APRPG-PEG-modified liposome encapsulating ADM on orthotopic pancreatic tumor model mice. Orthotopic pancreatic tumor model mice were injected *i.v.* with 0.3 M Glucose (control), PEG-LipADM or APRPG-PEG-LipADM for 4 times at day 3, 6, 9 and 12 after tumor implantation ($n=6$–8). Injected dose of liposomal ADM were adjusted to 10 mg/kg as ADM concentration in each time. The weight of the tumors was measured at day 15. Significant differences are shown with asterisks: *, $p<0.05$.

3.3. Intratumoral distribution of liposomes

Next, we determined intratumoral distribution of the liposomes in the present hypovascular tumor model. Three, nine and 18 days after tumor implantation, DiI C_{18}-labeled liposomes were injected *via* a tail vein of SUIT-2 orthotopically implanted mice. Two hours after injection, frozen section of tumor was prepared. After fluoroimmunostaing with CD31 antibody, the intratumoral distribution of liposomes was observed with confocal laser scan microscopy. As shown in Fig. 3a–c, red fluorescence indicating PEG-Lip localization was observed in vascular like structure of CD31-staining (green fluorescence). On the contrary, fluorescence of APRPG-PEG-Lip was observed not only in the vessel like structure but also with CD31-staining, suggesting that APRPG-PEG-Lip was associated with angiogenic endothelial cells.

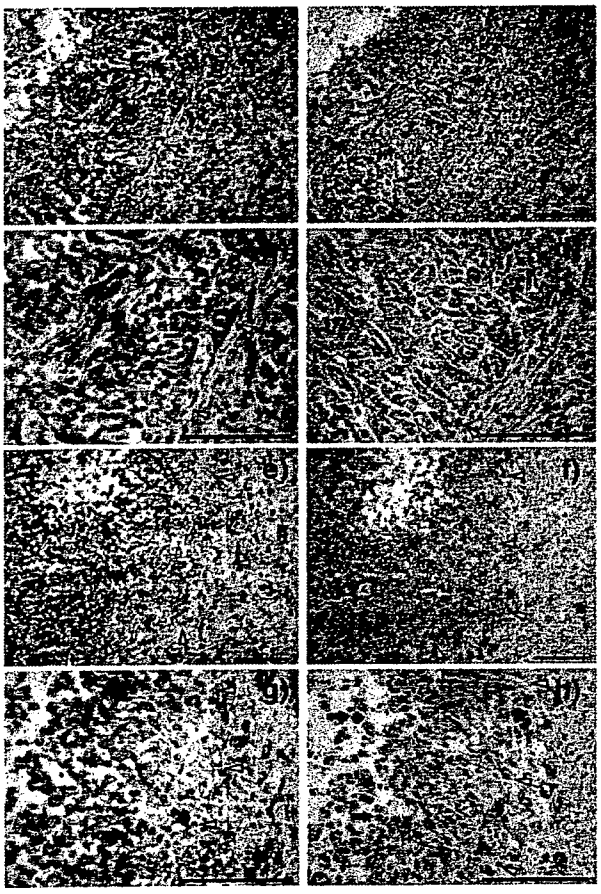

Fig. 5. Immunohistochemical analysis of dissected tumor after the treatment tumor model mice with APRPG-PEG-modified liposome encapsulating ADM. Orthotopic pancreatic tumor model mice were treated as described in the legend of Fig. 4. Tumor sections were prepared from the mice treated with PEG-LipADM (a–d) or with APRPG-PEG-LipADM (e–h). The sections were immunostained with biotinylated anti-mouse CD31 monoclonal antibody and visualized with DAB, and then co-stained with hematoxylin (a, c, e, g), or stained with hematoxylin-eosin (b, d, f, h). Arrowheads indicate the boundary of normal and tumor tissues, and arrows in (h) indicate macrophages. Scale bar represents 100 μm.

3.4. Therapeutic experiment by use of ADM-loaded liposomes

To examine the therapeutic effect of neovessel-targeted liposomal ADM on the orthotopic pancreatic tumor model mice, ADM-encapsulated APRPG-PEG-modified liposome (APRPG-PEG-LipADM) or ADM-encapsulated PEG-modified liposome (PEG-LipADM) were injected *via* a tail vein of the mice at 3, 6, 9 and 12 days after the tumor implantation. At day 15, tumor was removed and weighed to evaluate the effect of the treatment. As shown in Fig. 4, the significant differences in tumor weight of APRPG-PEG-LipADM-treated group from control ($p<0.05$) and PEG-LipADM-treated group ($p<0.05$) were observed. We also examined the body weight change of these mice after tumor implantation as an indicator of side effects, and observed that no significant difference between the three groups tested (data not shown).

Finally the sections of dissected tumor tissues were examined by immunostaining of CD31 and hematoxylin-eosin staining. As shown in Fig. 5, CD31-positive cells were observed in the tumor to some extent after treatment with PEG-LipADM. On the contrary, vessel-like structures were disappeared in the tumor after treatment with APRPG-PEG-LipADM, suggesting that APRPG-PEG-LipADM degenerated neovessels inside the tumor. Furthermore, the invasion of macrophages into the tumor was observed in the latter case.

4. Discussion

General anti-angiogenic therapy is based on the inhibition of the angiogenic cascade such as receptor binding of VEGF, signal transduction of VEGF, migration of proliferating endothelial cells, and tube formation. However, it is uncertain that the inhibition of angiogenic cascade is able to lead tumor regression. ANET is different from the traditional anti-angiogenic therapy, since this therapy eradicates proliferating endothelial cells and is expected to eradicate tumor cells through complete cutoff the blood supply to tumor tissues resulting in regression of the tumors. Moreover, ANET would not be expected to acquire drug-resistance, and would inhibit hematogenous metastases.

In here, we showed the therapeutic efficacies of ANET in orthotopic pancreatic tumor model by using tumor neovasculature-targeted liposome encapsulating an anti-cancer drug, ADM. Since pancreatic cancer is known as hypovascular cancer, injury of the small number of vascular cells may affect on large extent of cells that depend on supply of oxygen and nutrients to the vessel. Many experiments have been done to treat pancreatic tumor by anti-angiogenic therapy. These results, however, suggest that the effect of anti-angiogenic therapy alone is thought to be inadequate, concomitant treatments with anti-cancer drug or radiation have been tried [16,17]. On the other hand, ANET injures the proliferative angiogenic endothelial cells directly, and is expected to cause complete regression of tumor cells.

At first, we confirmed the model used here had characteristics of hypovascular tumor. As shown in Fig. 1, the CD31 positive area of orthotopic tumor model is significantly smaller

than that of s.c. implanted tumor. The efficiency of ANET in previous study was the case of s.c. implantation model [14]. The present study is for the first time to investigate whether ANET works in hypovascular tumor model. Biodistribution study by using ^{3}H-labeled PEG-Lip and APRPG-PEG-Lip showed no differences in the accumulation of liposome in the tumor. In general, PEG-modification prevents liposomes from opsonization and reticuloendothelial system (RES)-trapping [18]. This enables liposomes to circulate a long time in bloodstream and to accumulate in the interstitial spaces of tumor tissue through leaking out of angiogenic vessels: This behavior is due to so-called EPR effect [19,20], and such accumulation is called as passive targeting. APRPG peptide-modification adds an ability to actively interact with the angiogenic vessels, although the total accumulation of PEG-Lip and APRPG-PEG-Lip in the tumor was not significantly different. This result is consistent with our previous study using s.c. implanted tumor. We previously observed that the accumulation of PEG-Lip and APRPG-PEG-Lip was quite similar in s.c. implanted tumor model [14], but the intratumoral distribution was much different: PEG-Lip accumulated around angiogenic vessels, and APRPG-PEG-Lip associated with angiogenic vessels [15]. Therefore, we next determined the intratumoral distribution of the two liposomes by using confocal laser scan microscopy. On the other hand, biodistribution study showed the spleen and liver retention of liposomes. This retention is much lower than that of liposome without PEG-modification and the drug in them would show little effect on non-proliferative cells.

As shown in Fig. 3, APRPG-PEG-Lip and PEG-Lip were mainly distributed inside of vessel like structure after 2 h injection. Since these liposomes had long-circulating characteristics, they would effectively reach the vessel of the pancreatic tumor. Intravessel distribution of liposomes, however, was much different in these two kinds of liposomes. APRPG-PEG-Lip was colocalized with vessel marker CD31, although PEG-Lip was rather evenly distributed inside the vessel like structure. The accumulation of PEG-Lip at outside of vessels was not observed at this time point, although these vessels should be angiogenic vessels since APRPG-PEG-Lip having affinity to only neovessels associated with the vessels. The target of APRPG peptide is unclear at present, however, cellular uptake of APRPG-modified liposome significantly increased in VEGF-stimulated human umbilical vein endothelial cells (HUVECs) *in vitro* suggesting that some molecule which was expressed on the surface of the cells by the stimulation is responsible for the interaction. Moreover, a previous paper reported that one peptide including the PRP motif had an affinity for VEGF receptor [21]. Therefore, APRPG peptide may interact with endothelial cells through a certain molecule on the cell surface.

Finally, we examined the effect of ANET on the pancreatic tumor, and observed significant suppression of tumor growth by the treatment with APRPG-PEG-Lip encapsulating ADM. Since APRPG-PEG-Lip directly associated with growing angiogenic endothelial cells, ADM in the liposome might damage the angiogenic vessels. Generally, in pancreatic cancer, scirrhous gastric cancer and inflammatory breast cancer, drug carrier-based DDS require a long-distance transportation to get to the tumor cells which is a disadvantage for targeting DDS. PEG-Lip accumulated passively is thought to remain in large volume of stroma exists in pancreatic cancer, followed by poor anti-tumor activity. The APRPG-based anti-neovascular system may overcome this disadvantage by directly and effectively injuring targeted proliferative angiogenic vessels. Immunohistochemical analysis also supported the idea.

In conclusion, ANET has the possibility to treat hypovascular pancreatic tumor by injuring the neovessels. APRPG-modification of PEG-Lip endows it with binding ability to angiogenic endothelial cells, therefore ADM encapsulated in the liposome may effectively damage the cells, which causes enhanced therapeutic efficacy compared to that by ADM in PEG-Lip. Since PEG-Lip accumulated in orthotopic pancreatic tumor in a similar extent to APRPG-PEG-Lip, the inferior therapeutic efficacy of ADM in PEG-Lip to that in APRPG-PEG-Lip might be due to the topological distribution difference: PEG-Lip might reside in the interstitial spaces of the tumor, and gradually release ADM which causes damage of growing cells.

References

[1] A. Jemal, T. Murray, A. Samuels, A. Ghafoor, E. Ward, M.J. Thun, Cancer statistics, CA Cancer J. Clin. 53 (1) (2003) 5–26.
[2] D.R. Martin, R.C. Semelka, MR imaging of pancreatic masses, Magn. Reson. Imaging Clin. N. Am. 8 (4) (2000) 787–812.
[3] J. Rosai, in: J. Rosai (Ed.), Ackerman's Surgical Pathology, 8th ed, Mosby, St. Louis, 1996, pp. 969–1013.
[4] R.C. Semelka, L.L. Nagase, D. Armao, et al., in: R.C. Semelka (Ed.), Abdominal-Pelvic MRI, 2nd ed, Wiley–Liss, New York, 2002, pp. 373–490.
[5] C.J. Bruns, C.C. Solorzano, M.T. Harbison, S. Ozawa, R. Tsan, D. Fan, J. Abbruzzese, P. Traxler, E. Buchdunger, R. Radinsky, I.J. Fidler, Blockade of the epidermal growth factor receptor signaling by a novel tyrosine kinase inhibitor leads to apoptosis of endothelial cells and therapy of human pancreatic carcinoma, Cancer Res. 60 (11) (2000) 2926–2935.
[6] R.G. Chirivi, A. Garofalo, M.J. Crimmin, L.J. Bawden, A. Stoppacciaro, P.D. Brown, R. Giavazzi, Inhibition of the metastatic spread and growth of B16-BL6 murine melanoma by a synthetic matrix metalloproteinase inhibitor, Int. J. Cancer 58 (3) (1994) 460–464.
[7] S.A. Eccles, G.M. Box, W.J. Court, E.A. Bone, W. Thomas, P.D. Brown, Control of lymphatic and hematogenous metastasis of a rat mammary carcinoma by the matrix metalloproteinase inhibitor batimastat (BB-94), Cancer Res. 56 (12) (1996) 2815–2822.
[8] H. Hurwitz, L. Fehrenbacher, W. Novotny, T. Cartwright, J. Hainsworth, W. Heim, J. Berlin, A. Baron, S. Griffing, E. Holmgren, N. Ferrara, G. Fyfe, B. Rogers, R. Ross, F. Kabbinavar, Bevacizumab plus irinotecan, fluorouracil, and leucovorin for metastatic colorectal cancer, N. Engl. J. Med. 350 (23) (2004) 2335–2342.
[9] B.A. Teicher, N.P. Dupuis, M.F. Robinson, Y. Emi, D.A. Goff, Antiangiogenic treatment (TNP-470/minocycline) increases tissue levels of anticancer drugs in mice bearing Lewis lung carcinoma, Oncol. Res. 7 (5) (1995) 237–243.
[10] H. Satoh, H. Ishikawa, M. Fujimoto, M. Fujiwara, Y.T. Yamashita, T. Yazawa, M. Ohtsuka, S. Hasegawa, H. Kamma, Angiocytotoxic therapy in human non-small cell lung cancer cell lines-advantage of combined effects of TNP-470 and SN-38, Acta Oncol. 37 (1) (1998) 85–90.
[11] N. Oku, T. Asai, K. Watanabe, K. Kuromi, M. Nagatsuka, K. Kurohane, H. Kikkawa, K. Ogino, M. Tanaka, D. Ishikawa, H. Tsukada, M. Momose, J. Nakayama, T. Taki, Anti-neovascular therapy using novel peptides homing to angiogenic vessels, Oncogene 21 (17) (2002) 2662–2669.
[12] T. Asai, M. Nagatsuka, K. Kuromi, S. Yamakawa, K. Kurohane, K. Ogino, M. Tanaka, T. Taki, N. Oku, Suppression of tumor growth by novel peptides homing to tumor-derived new blood vessels, FEBS Lett. 510 (3) (2002) 206–210.